Cell

Resource

The Q System: A Repressible Binary System for Transgene Expression, Lineage Tracing, and Mosaic Analysis

Christopher J. Potter,[1,2,4,5] Bosiljka Tasic,[1,2,4] Emilie V. Russler,[1,2] Liang Liang,[1,2,3] and Liqun Luo[1,2,*]
[1]Howard Hughes Medical Institute
[2]Department of Biology
[3]Department of Applied Physics
Stanford University, Stanford, CA 94305, USA
[4]These authors contributed equally to this work
[5]Present address: Center for Sensory Biology, The Solomon H. Snyder Department of Neuroscience, Johns Hopkins University School of Medicine, 855 North Wolfe Street, Baltimore, MD 21205, USA
*Correspondence: lluo@stanford.edu
DOI 10.1016/j.cell.2010.02.025

SUMMARY

We describe a new repressible binary expression system based on the regulatory genes from the *Neurospora qa* gene cluster. This "Q system" offers attractive features for transgene expression in *Drosophila* and mammalian cells: low basal expression in the absence of the transcriptional activator QF, high QF-induced expression, and QF repression by its repressor QS. Additionally, feeding flies quinic acid can relieve QS repression. The Q system offers many applications, including (1) intersectional "logic gates" with the GAL4 system for manipulating transgene expression patterns, (2) GAL4-independent MARCM analysis, and (3) coupled MARCM analysis to independently visualize and genetically manipulate siblings from any cell division. We demonstrate the utility of the Q system in determining cell division patterns of a neuronal lineage and gene function in cell growth and proliferation, and in dissecting neurons responsible for olfactory attraction. The Q system can be expanded to other uses in *Drosophila* and to any organism conducive to transgenesis.

INTRODUCTION

The ability to introduce engineered transgenes with regulated expression into organisms has revolutionized biology. A popular strategy for regulating expression of an effector transgene is to use a binary expression system. In this strategy, one transgene contains a specific promoter driving an exogenous transcription factor, while the other transgene uses the promoter activated only by that transcription factor to drive the effector gene. As a result, the effector gene is controlled exclusively by the chosen transcription factor, and the expression pattern of the effector transgene corresponds to the expression pattern of the exogenous transcription factor (Figure 1A). A number of binary expression systems have been established in genetic model organisms, including tetracycline-regulable tTA/TRE in mice (Gossen and Bujard, 1992) and GAL4/UAS in flies (Fischer et al., 1988; Brand and Perrimon, 1993). Compared to effector transgenes driven directly by a promoter, binary systems offer several advantages. First, binary systems usually result in higher levels of effector transgene expression as a result of transcription factor-mediated amplification. Second, expression of some effectors directly by a promoter may cause lethality and thus prevent the generation of viable transgenic animals; in binary systems, the effector transgene is not expressed until the exogenous transcription factor is introduced into the same animal, usually through a genetic cross. Third, some transcription factors used in binary systems can be additionally regulated by small molecule ligands and thus offer temporal control of transgene expression. Lastly, libraries of transgenes expressing a transcription factor and/or corresponding effectors can be established, such that the transcription factor and effector transgenes can be systematically combined by genetic crosses to enable expression of the same effector transgene in different patterns, or different effector transgenes in the same pattern, thereby enabling a variety of genetic screens in vivo.

The impact of the budding yeast-based GAL4/UAS binary expression system on studies of *Drosophila* biology cannot be overstated. Thousands of GAL4 lines have been characterized for expression in specific tissues and developmental stages (Brand and Perrimon, 1993; Hayashi et al., 2002; Pfeiffer et al., 2008). Tens of thousands of UAS-effector lines have also been established (Rørth et al., 1998), including a UAS-RNAi library against most predicted genes in the *Drosophila* genome (Dietzl et al., 2007). Moreover, the finding that the yeast repressor of GAL4, GAL80, efficiently represses GAL4-induced transgene expression in *Drosophila* (Lee and Luo, 1999) offered additional control of the system. For example, in combination with FLP/FRT-mediated mitotic recombination (Golic and Lindquist, 1989; Xu and Rubin, 1993), GAL80/GAL4/UAS can be used to create mosaic animals via MARCM (mosaic analysis with

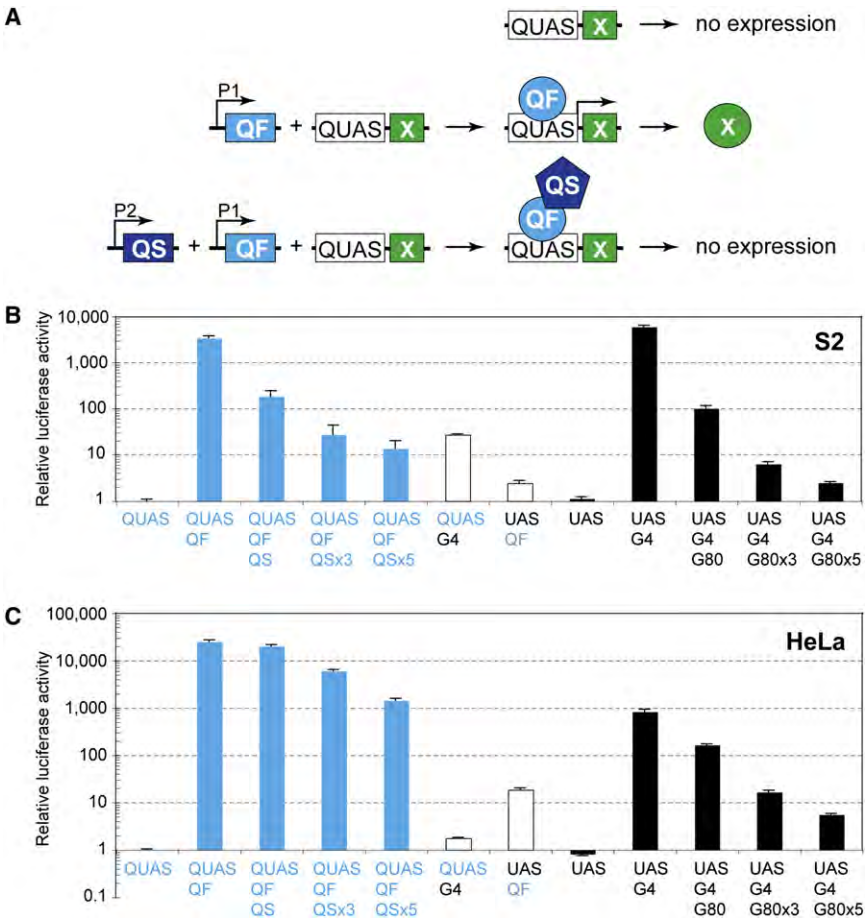

Figure 1. Characterization of the Q System in *Drosophila* and Mammalian Cells

(A) Schematic of the Q repressible binary expression system. In the absence of the transcription factor, QF, the QF-responsive transgene, *QUAS-X*, does not express X (top). When *QF* and *QUAS-X* transgenes are present in the same cell where QF is expressed (promoter P1 is active), QF binds to *QUAS* and activates expression of transgene X (middle). When *QS*, *QF*, and *QUAS-X* transgenes are present in the same cell, and both P1 and P2 promoters are active, QS represses QF and X is not expressed (bottom).

(B) Characterization of the Q system in transiently transfected *Drosophila* S2 cells. Relative luciferase activity (normalized as described in the Extended Experimental Procedures) is plotted on a logarithmic scale on the y axis, with *QUAS-luc2* alone set to 1. Error bars represent the standard error of the mean (SEM). Plasmids used for transfections are noted below the x axis. QUAS, *pQUAS-luc2* reporter; QF, *pAC-QF*; QS, *pAC-QS*; UAS, *pUAS-luc2* reporter; G4, *pAC-GAL4*; G80, *pAC-GAL80*; x3 and x5, 3- and 5-fold molar excess of QS over QF or GAL80 over GAL4.

(C) Characterization of the Q system in transiently transfected human HeLa cells. Explanations and abbreviations are as in (B), except as follows: QF, *pCMV-QF*; QS, *pCMV-QS*; G4, *pCMV-GAL4*; G80, *pCMV-GAL80*.

Figure S1 shows the effects of quinic acid on the Q and GAL4 systems in cultured cells.

a repressible cell marker) (Lee and Luo, 1999). With MARCM, mosaic animals can be created that contain a small population of genetically defined cells labeled by a transgenic marker (such as GFP). At the same time, these labeled cells can be homozygous mutant for a gene of interest and/or modified with additional effector transgenes. MARCM has been widely used for lineage analysis, for tracing neural circuits, and for high-resolution mosaic analysis of gene function (Luo, 2007).

The versatile GAL4/UAS system still has limitations. The GAL4 expression patterns from enhancer trap lines or promoter-driven transgenes often include cells other than the cells of interest. It is thus difficult to assign the effect of transgene expression to a specific cell population, especially when phenotypes, such as behavior, are assayed at the whole organism level. Additionally, analysis of gene function and dissection of complex biological systems in multicellular organisms often requires independent genetic manipulations of separate populations of cells. For the improvement of the precision of transgene expression, intersectional expression methods such as the split GAL4 system (Luan et al., 2006) or the combined use of GAL4/UAS and FLP/FRT (Stockinger et al., 2005) have been introduced. To enable independent manipulation of separate populations of cells, additional binary systems such as the lexA/lexAO system have been developed (Lai and Lee, 2006). Here, we describe a new repressible and small molecule-regulable binary expression system, the Q system, which offers significant advantages and versatility compared to the existing systems.

The Q system utilizes regulatory genes from the *Neurospora crassa qa* gene cluster. This cluster consists of five structural genes and two regulatory genes (*qa-1F* and *qa-1S*) used for the catabolism of quinic acid as a carbon source (Giles et al., 1991). QA-1F (shortened as QF hereafter) is a transcriptional activator that binds to a 16 bp sequence present in one or more copies upstream of each *qa* gene (Patel et al., 1981; Baum et al., 1987). QA-1S (shortened as QS hereafter) is a repressor of QF that blocks its transactivation activity (Huiet and Giles, 1986) (Figure 1A). Here, we explore the properties of the Q system in cultured fly and mammalian cells, and demonstrate its utility for transgene expression, lineage tracing and genetic mosaic analysis in *Drosophila* in vivo.

RESULTS AND DISCUSSION

Characterization of the Q System in *Drosophila* and Mammalian Cells

To test whether *qa* cluster genes function in biological systems besides *Neurospora*, we created expression constructs for transient transfection of *Drosophila* and mammalian cells. We used the same ubiquitous promoters to drive QF and QS: *actin 5c* for *Drosophila* and CMV for mammalian cells. We generated

a reporter plasmid containing the synthetic firefly luciferase (*luc2*) gene under the control of five copies of the QF binding site, which we termed QUAS, and the *Drosophila hsp70* minimal promoter. We also created the GAL4 system equivalents as controls and for quantitative comparisons with the Q system.

Transfection of *Drosophila* S2 cells with *QF* and *QUAS-luc2* resulted in ~3300-fold enhancement of luc2 expression compared with *QUAS-luc2* alone (Figure 1B). For comparison, GAL4 induced luc2 expression from *UAS-luc2* by ~5300-fold (Figure 1B) and therefore had ~1.6-fold higher inducibility than QF/QUAS. GAL4/UAS also reached ~1.8-fold higher level of reporter expression than QF/QUAS. Cotransfection of *QS* with *QF* and *QUAS-luc2* resulted in dosage-dependent suppression of luc2 expression (Figure 1B). Full suppression was not observed with equimolar ratios of QF and QS (similar lack of full suppression was observed with GAL4/GAL80). Quinic acid, which relieves suppression of QS in *Neurospora* (Giles et al., 1991), significantly suppressed QS to restore QF-based transcription (Figure S1A available online). Finally, QF and GAL4 showed minimal cross-activation of *UAS* and *QUAS*, respectively (Figure 1B, middle)—QF activation of *UAS* was ~1500-fold less than that of *QUAS*; GAL4 activation of *QUAS* was ~200-fold less than that of *UAS*.

In human HeLa cells (Figure 1C), the Q system behaved similarly as in *Drosophila* S2 cells, but with the following distinctions. First, QF induced expression from *QUAS* by ~24,000-fold, compared to ~1000-fold induction of *UAS* by GAL4. Therefore, in human cells, QF/QUAS achieves ~24-fold higher inducibility and ~30-fold higher level of reporter expression than GAL4/UAS. Second, higher QS:QF or GAL80:GAL4 molar ratios are required for effective suppression in HeLa cells compared with *Drosophila* S2 cells. Third, quinic acid does not suppress QS in mammalian cells, but seems to activate it further to make it an even better repressor (Figure S1B); the reasons for this unexpected behavior in mammalian cells are unknown. All these distinctions were also observed in COS cells (data not shown). Taken together, these experiments demonstrate that the Q repressible binary expression system is effective in *Drosophila* and mammalian cells.

Repressible Binary Transgene Expression with the Q System in *Drosophila* In Vivo

To test whether the Q system functions in *Drosophila* in vivo, we generated transgenic flies that express (1) different markers under the control of *QUAS*, (2) *QF* under the control of a specific promoter or in enhancer trap vectors, and (3) *QS* under the control of a ubiquitous tubulin promoter (*tubP-QS*) (Table S1).

Figures 2A and 2B (left panels) show low basal fluorescence in whole mount *Drosophila* adult brains harboring only reporter transgenes, *QUAS-mCD8-GFP* (full-length mouse CD8 followed by GFP) or *QUAS-mtdT-HA* (myristoylated and palmitoylated tandem dimer Tomato followed by three copies of the HA epitope). The low basal expression of *QUAS* and *UAS* reporters provides significant advantage over the lexA binary expression system (Lai and Lee, 2006). All *QUAS-mCD8-GFP* transgenic flies have basal reporter expression comparable to or lower than the *lexO-mCD2-GFP* line with the lowest reporter expression (Figure S2A). Low basal expression was also observed in other *QUAS* reporters such as *QUAS-mdtT-HA* (Figure S2A, data not shown). These observations suggest that the *QUAS* promoter is not easily influenced by genomic enhancers near the transgene insertion site and that flies do not contain endogenous proteins capable of inducing significant expression from *QUAS*-transgenes at least within the tissues we examined.

Introduction of transgenes expressing QF into flies containing *QUAS*-markers results in strong marker expression. For example, QF driven by the *GH146* enhancer (Stocker et al., 1997; Berdnik et al., 2008) drives strong reporter gene expression in olfactory projection neurons (PNs; Figures 2A_2, 2A_3, 2B_2, and 2B_3). We also isolated enhancer trap lines that drive strong reporter expression in imaginal discs and adult tissues including large subsets of neurons and glia (Figure 2C, middle; Figures S2B and S3). Expression of these transgenes was effectively suppressed by ubiquitous expression of QS (Figures 2A_4, 2B_4, and 2C, right; Figure S2B). These experiments show that the Q repressible binary system is as effective in vivo as the widely used GAL80/GAL4/UAS system (Brand and Perrimon, 1993; Lee and Luo, 1999).

The Q system provides an additional level of control compared to the GAL4 system: inhibition of QS by quinic acid. Addition of increasing doses of quinic acid to fly food on which flies developed increasingly reverted the QS inhibition of enhancer trap *ET40-QF* driven *QUAS-mtdT-HA* expression (Figure 2D). When adult flies were transferred to quinic acid-containing food, reversion of suppression could be seen after 6 hr, with marked reversion after 24 hr and saturation by day 5 (Figure 2E, data not shown). Flies kept for nine generations on food containing high doses of quinic acid, a natural product present at >1% in cranberry juice (Nollet, 2000), exhibited no noticeable abnormalities. Quinic acid can thus be used to temporally regulate QF-driven transgene expression. For instance, one can suppress developmental expression of a transgene and allow reactivation in adult for behavioral analysis, analogously to the $GAL80^{ts}$ strategy (McGuire et al., 2003). This manipulation can be achieved without changing the temperature, thereby avoiding complications with temperature-sensitive behaviors.

Q-MARCM

An incentive to develop the Q repressible binary system is the potential to build a new GAL4-independent MARCM system. The Q system-based MARCM (Q-MARCM) can then be used to mark and genetically manipulate a single cell or a small population of cells, while GAL4/UAS can be used to genetically manipulate a separate population of cells in the same animal. To test Q-MARCM, we placed *tubP-QS* distally to an FRT site and used FLP/FRT to induce mitotic recombination, so that one of the two daughter cells would lose *tubP-QS*, thus permitting QF to drive *QUAS-marker* expression (Figure 3A).

Using *GH146-QF* to label olfactory PNs in Q-MARCM experiments, we found single-cell and neuroblast clones labeled by *QUAS-mCD8-GFP* (Figure 3B) or *QUAS-mtdT-HA* (see below). In single-cell clones, the dendritic innervation of individual glomeruli in the antennal lobe and stereotyped projections of single axons in the lateral horn appeared indistinguishable from previously characterized single-cell clones labeled by GH146-GAL4-based MARCM (Jefferis et al., 2001; Marin et al., 2002;

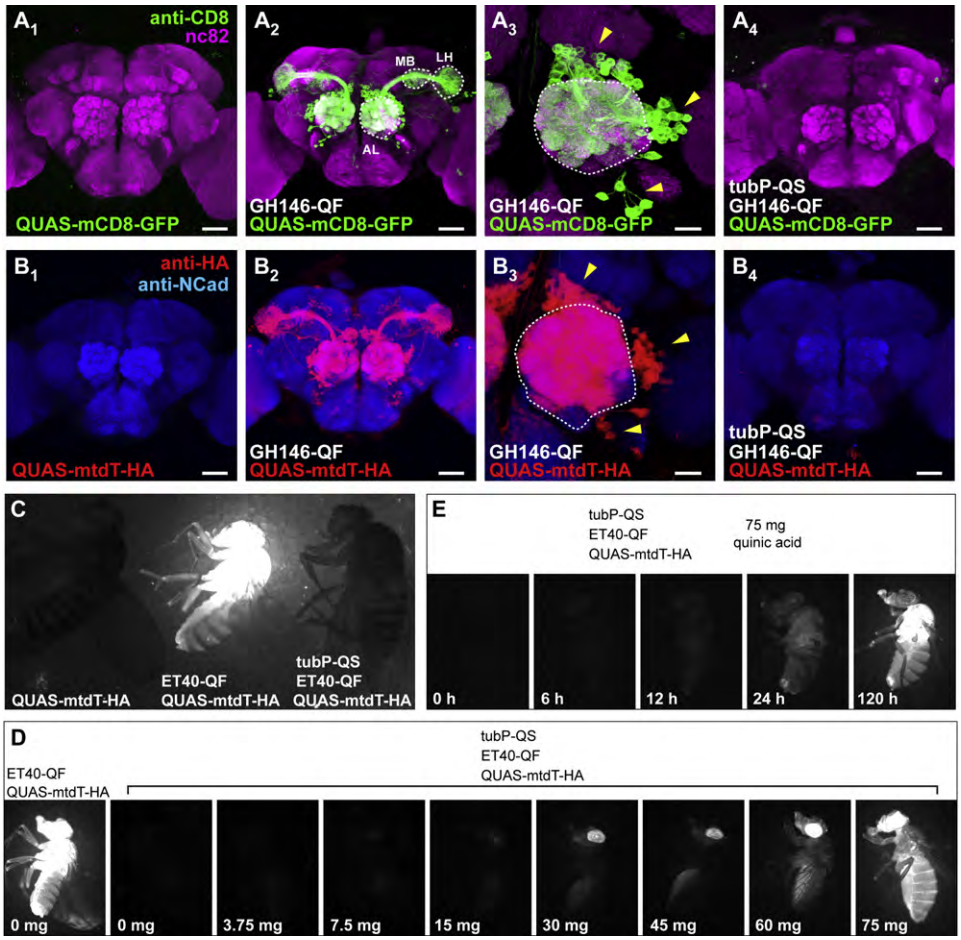

Figure 2. In Vivo Characterization of the Q system in Flies

(A) Representative confocal projections of whole-mount *Drosophila* brains immunostained for a general neuropil marker (monoclonal antibody nc82) in magenta, and for mCD8 in green. Genotypes are indicated at the bottom. (A_3) is a higher-magnification image centered at the antennal lobe (AL; outlined). QF is driven by the *GH146* enhancer that labels a large subset of olfactory projection neurons (PNs). PN cell bodies (arrowheads in A_3) are located in anterodorsal, lateral or ventral clusters around the AL. PNs project dendrites into the AL, and axons to the mushroom body calyx (MB) and the lateral horn (LH) (outlined). The green channel for (A_1) and (A_4) was imaged under the same gain, which is 15% higher than for the images shown in (A_2) and (A_3).

(B) Representative confocal projections of whole-mount *Drosophila* brains immunostained for a general neuropil marker N-cadherin in blue, and for HA in red. The genotypes are indicated at the bottom. (B_3) is a higher-magnification image centered at the AL (outlined). Arrowheads denote PN cell bodies. The red channel for (B_1) and (B_4) was imaged under the same gain, which is 15% higher than for the images shown in (B_2) and (B_3). The red signal in (B_4) is due to the DsRed transgenic marker associated with the *GH146-QF* transgene vector.

(C) Fluorescence images of three adult flies with genotypes as indicated.

(D) Fluorescence images of adult flies with genotypes indicated on top. Numbers on the bottom indicate the amount of quinic acid (dissolved in 300 μl water) added to the surface of ~10 ml fly food, on which these flies developed.

(E) Fluorescence images of adult flies showing time course of derepression of QS by quinic acid. The adult flies of the genotype listed on top were moved from vials with regular food to vials containing 75 mg quinic acid and imaged after the time interval shown on the bottom.

Scale bars represent 50 μm in (A_1), (A_2), (A_4), (B_1), (B_2), and (B_4) and 20 μm in (A_3) and (B_3). Figures S2 and S3 characterize additional *QUAS* reporters and *QF* enhancer trap lines.

Jefferis et al., 2007). We have validated *tubP-QS* transgenes on all five major chromosome arms (Table S1), thereby allowing GAL4-independent MARCM analysis for a vast majority of *Drosophila* genes using the Q system.

GAL4 and QF showed minimal cross-activation of their respective upstream activating sequences in cultured cells (Figures 1B and 1C). Moreover, we could not detect any cross-activation (Figure S4A) or cross-repression (Figure S4B) of the GAL4 and QF systems in vivo. Therefore, QF- and GAL4-based MARCM (G-MARCM) can be combined in the same fly. If *tubP-GAL80* and *tubP-QS* are placed distally to FRT sites on different chromosome arms (Figure S4C), independently generated clones can be labeled by Q- and G-MARCM. This arrangement, which we term ''independent double MARCM,'' can be used to study interactions between two separate populations of cells that have undergone independent mitotic recombination and genetic alteration. If *tubP-GAL80* and *tubP-QS* transgenes are placed distally to the same FRT site in *trans* (Figure 3C), sister

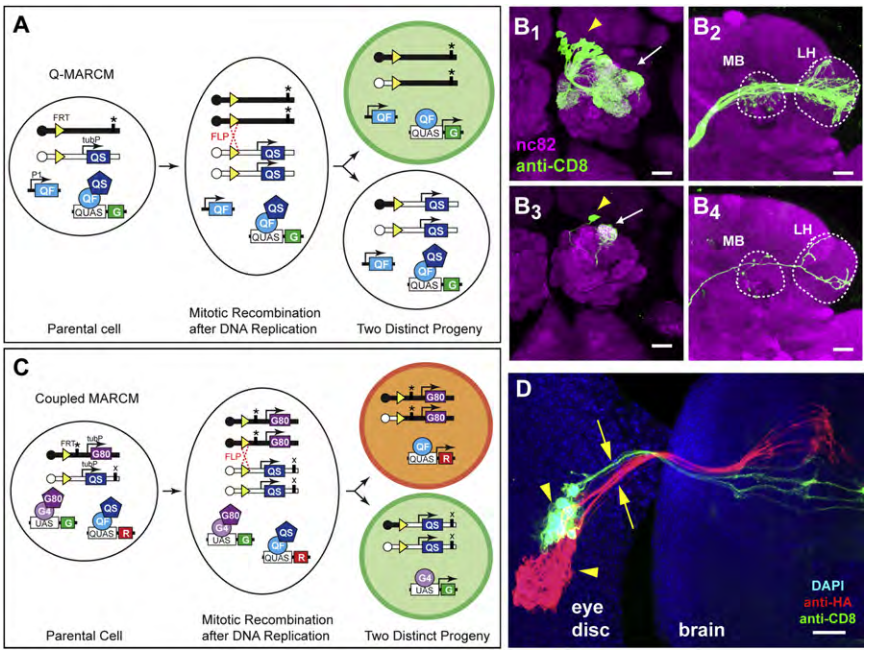

Figure 3. Q-MARCM and Coupled MARCM

(A) Scheme for Q-MARCM. FLP/FRT-mediated mitotic recombination in G2 phase of the cell cycle (dotted red cross) followed by chromosome segregation as shown causes the top progeny to lose both copies of *tubP-QS*, and thus becomes capable of expressing the GFP marker (G) activated by QF. It also becomes homozygous for the mutation (*). *QF* and *QUAS* reporter transgenes can be located on any other chromosome arm. P1, promoter 1; tubP, tubulin promoter. Centromeres are represented as circles on chromosome arms.

(B) Q-MARCM clones of olfactory PNs visualized by *GH146-QF* driven *QUAS-mCD8-GFP*.

(B_1 and B_2) Confocal images of an anterodorsal neuroblast clone showing cell bodies of PNs (arrowhead), their dendritic projections in the antennal lobe (arrows) and axonal projections in the MB and LH (outlined).

(B_3 and B_4) Confocal images of a single cell clone showing the cell body of a DL1 PN (arrowhead), its dendritic projection into the DL1 glomerulus (arrow) of the antennal lobe and its axonal projection in the MB and LH (outlined).

(C) Scheme for coupled MARCM. The *tubP-GAL80* and *tubP-QS* transgenes are distal to the same FRT on homologous chromosomes. Mitotic recombination followed by specific chromosome segregation produces two distinct progeny devoid of *QS* or *GAL80* transgenes, respectively, and therefore capable of expressing red (R) or green (G) fluorescent proteins, respectively. *QF* and *GAL4* transgenes (not diagramed), as well as *QUAS* and *UAS* transgenes, can be located on any other chromosome arm. "*" and "x" designate two independent mutations that can be rendered homozygous in sister progeny.

(D) A coupled MARCM clone of photoreceptors, showing clusters of cell bodies (arrowheads) in the eye imaginal disc and their axonal projections (arrows) to the brain. The green clone was labeled by *tubP-GAL4* driven *UAS-mCD8-GFP*; the red clone was labeled by *ET40-QF* driven *QUAS-mtdT-HA*. Blue, DAPI staining for nuclei. Image is a Z projection of a confocal stack.

Scale bars represent 20 μm. Figure S4 shows the lack of cross-activation and cross-repression of the Q and GAL4 systems in vivo and a schematic of independent double MARCM.

cells resulting from the same mitotic recombination can be labeled by Q- and G-MARCM respectively. We call the latter case "coupled MARCM."

Figure 3D illustrates an example of coupled MARCM in the third-instar larval eye disc. Sister cells and their descendants, derived from a single mitotic recombination event based on clone frequency and the proximity of labeled cells, are marked by *tubP-GAL4* driven *UAS-mCD8-GFP* and *ET40-QF* driven *QUAS-mtdT-HA*. The photoreceptor cell bodies and their axonal projections into the brain were clearly visualized by both G-MARCM and Q-MARCM.

Analysis of Lineage and Cell Division Patterns with Coupled MARCM

The ability to label both progeny of a dividing cell with different colors via coupled MARCM (Figure 3C) can be used to characterize two important aspects of a developmental process: cell lineage and division patterns. As an example to illustrate such utility, we investigated the cell division pattern of a central nervous system neuroblast that gives rise to a subset of adult olfactory PNs.

The cell division patterns of neuroblasts that generate adult insect central nervous system (CNS) neurons are thought to follow the scheme shown in Figure 4A: a neuroblast undergoes asymmetric divisions to produce a new neuroblast and a ganglion mother cell (GMC), which divides once more to produce two postmitotic neurons (Nordlander and Edwards, 1969). A previous GAL4-based MARCM analysis of the mushroom body lineage supports this model: neuroblast, two-cell, and single-cell clones can be produced (Figure 4B), and the frequency of the neuroblast and two-cell clones is roughly equal, reflecting the random segregation of the GAL80-containing chromosomes into the neuroblast or the GMC (Lee et al., 1999; Lee and Luo, 1999). However, when we analyzed PN lineages using MARCM and *GH146-GAL4* (Jefferis et al., 2001) or *GH146-QF* (data not shown), we obtained either neuroblast or single-cell clones, but no two-cell PN clones. Three different models can account for these data (Figure 4C). In model I, the stereotypical division pattern (Figure 4A) does not apply to this lineage: GH146-positive PNs are direct descendants of the neuroblasts. In models II and III, the general division pattern still applies, but the sibling for the GH146-positive PN either is a GH146-negative cell (model II) or dies (model III).

We used coupled MARCM to distinguish among these models, focusing on the best-characterized anterodorsal lineage in which all progeny are PNs (Lai et al., 2008) and where birth order has been determined for most GH146-positive PNs (Jefferis et al., 2001; Marin et al., 2005). We used *GH146-QF* to label PNs derived from one progeny of a cell division, and the ubiquitous *tubP-GAL4* to label the sibling progeny (Figure S5). We

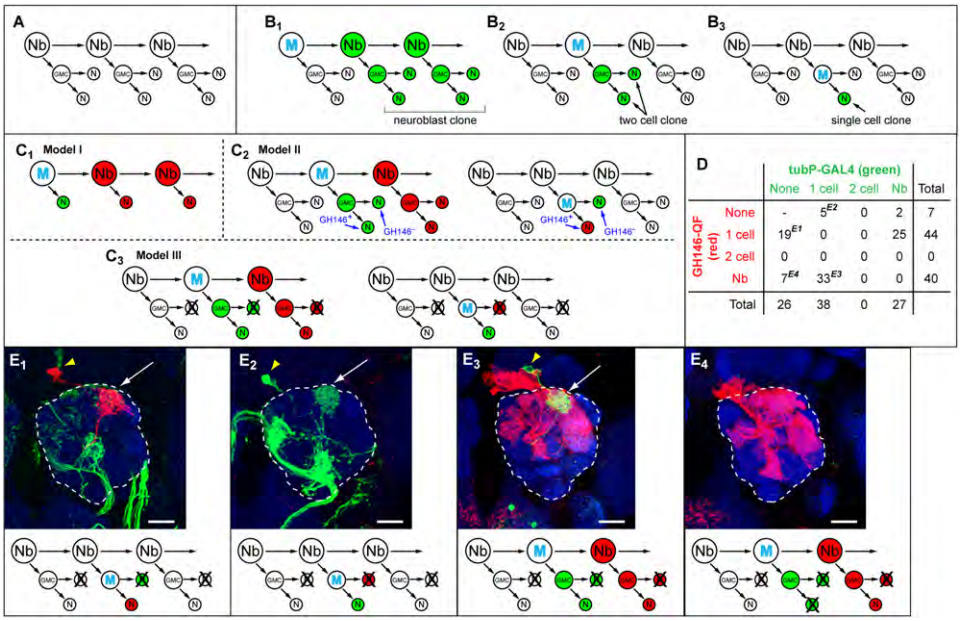

Figure 4. Lineage Analysis with Coupled MARCM

(A) General scheme for neuroblast division in the insect CNS. Nb, neuroblast; GMC, ganglion mother cell; N, postmitotic neuron.

(B) Three types of MARCM clones predicted from the general scheme. M, mitotic recombination.

(C) Three models to account for the lack of two cell clones in GH146-labeled MARCM. In (C_1), each neuroblast division directly produces a postmitotic GH146-positive PN without a GMC intermediate. In (C_2), each GMC division produces a GH146-positive PN and a GH146-negative cell. In (C_3), each GMC division produces a GH146-positive PN and a sibling cell that dies. For models II and III, simulations of coupled MARCM results are shown for mitotic recombination that occurs either in the neuroblast or in the GMC.

(D) Tabulation of coupled MARCM results. Superscripts next to the numbers correspond to the images shown in (E) as examples.

(E) Examples of coupled MARCM that contradict models I and II, but can be accounted for by model III (bottom). (E_1) and (E_2) show a single QF- (E_1) or GAL4- (E_2) labeled PN in the absence of labeled siblings. These events contradict model I (C_1). In both examples, the additional green staining in the antennal lobe belongs to *tubP-GAL4*-labeled axons from olfactory receptor neurons. (E_3) shows single *tubP-GAL4*-labeled sibling (green) of a *GH146-QF*-labeled neuroblast clone (red). This observation contradicts model II (C_2). (E_4) shows an occasional QF-labeled neuroblast clone with no *tubP-GAL4*-labeled siblings. All images are Z projections of confocal stacks. Green, anti-CD8 staining for *UAS-mCD8-GFP*; red, anti-HA staining for *QUAS-mtdT-HA*; blue, neuropil markers; arrowheads, PN cell bodies; arrows, dendritic innervation in the antennal lobe (outlined).

Scale bars represent 20 μm. See Figure S5 for a schematic for these coupled MARCM experiments.

induced clones by heat shock at different time windows within 0–100 hr after egg laying and recovered a total of 91 coupled MARCM clones. We sorted the clones according to their labeling by *GH146-QF* and *tubP-GAL4* (Figure 4D).

If model I were true, a single PN should always have a neuroblast sibling (Figure 4C_1). However, we found 19 out of 44 single PNs labeled by *GH146-QF* without a *tubP-GAL4*-labeled neuroblast clone (Figure 4D; Figure 4E_1) and five out of 38 single PNs labeled by *tubP-GAL4* without a *GH146-QF*-labeled neuroblast clone (Figure 4D; Figure 4E_2). Thus, model I does not apply.

If model II were true, *GH146-QF*-labeled neuroblast clones should be coupled with a two-cell clone labeled by the ubiquitous *tubP-GAL4* (regardless of them being GH146 positive or GH146 negative; Figure 4C_2, left). However, of the 40 *GH146-QF*-labeled neuroblast clones, none of the *tubP-GAL4*-labeled siblings were two-cell clones (Figure 4D). Instead, in 33 cases, the siblings were single-cell clones (Figure 4E_3), and in the other seven cases, there were no labeled siblings (Figure 4E_4). In addition, model II would predict pairs of sister cells each labeled by *tubP-GAL4* or *GH146-QF* as a result of mitotic recombination in the GMC (Figure 4C_2, right), but such an event was never observed (Figure 4D).

These experiments therefore support model III: the sibling of each PN dies during development and is no longer present in the adult brain (Figure 4C_3). The frequent occurrence of single singly labeled PNs without labeled siblings could result from mitotic recombination in the GMC giving rise to two cells, one of which dies (bottom of Figures 4E_1 and 4E_2). In addition, occasionally both GMC-derived siblings may die, giving rise to neuroblast clones without any labeled siblings (Figure 4E_4). This model is also supported by a recent study using different methods (Lin et al., 2010). It is possible that the division patterns producing PNs vary at different developmental stages and for different lineages. Future systematic studies using coupled MARCM can provide a comprehensive description of lineage and cell division patterns in these and other neuroblast lineages and can create a developmental history for neurons of the adult *Drosophila* brain.

Comparisons with Other Methods

While this manuscript was in preparation, two other twin-spot labeling methods were reported. "Twin-spot MARCM" uses

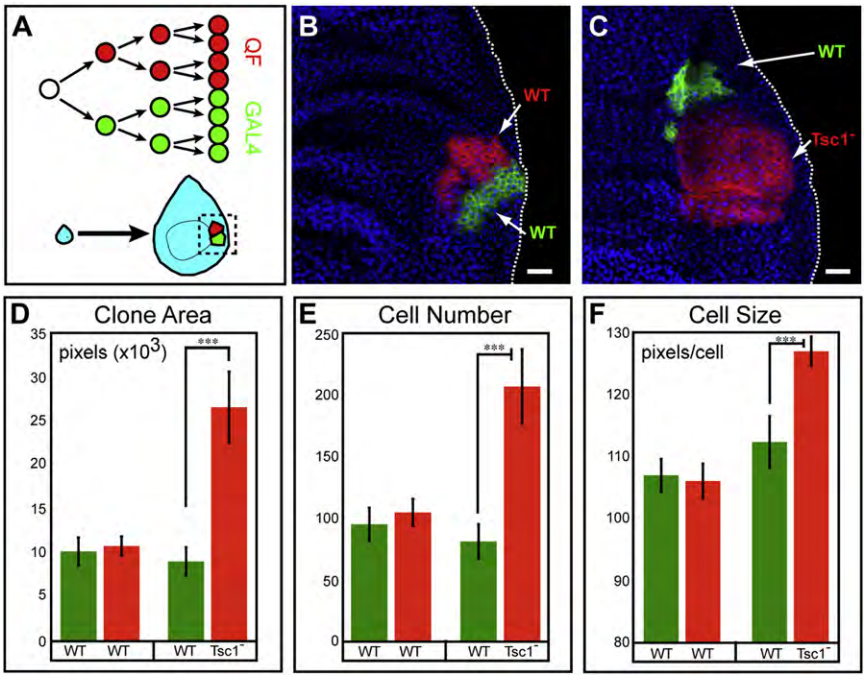

Figure 5. Coupled MARCM for Clonal Analysis of Mutant Phenotypes

(A) Schematic for coupled MARCM labeling of dividing cells during imaginal disc development.

(B) A control coupled MARCM clone. Both GAL4- and QF-labeled siblings are wild-type. Genotype: *hsFLP, QUAS-mtdT-HA, UAS-mCD8-GFP (X); ET40-QF, QUAS-mtdT-HA/+ (II); tubP-GAL4, 82B^{FRT}, tubP-GAL80/82B^{FRT},tubP-QS (III).*

(C) A coupled MARCM clone where GAL4-labeled sibling (green) is wild-type, while QF-labeled sibling (red) is homozygous mutant for *Tsc1*. Genotype: *hsFLP, QUAS-mtdT-HA, UAS-mCD8-GFP (X); ET40-QF, QUAS-mtdT-HA/+ (II); tubP-GAL4, 82B^{FRT}, tubP-GAL80, Tsc1^{Q600X} /82B^{FRT}, tubP-QS (III).*

(B and C) Green, anti-CD8; red, anti-HA; blue, anti-fibrillarin (labels nucleoli). Scale bars represent 20 μm.

(D–F) Quantification of clone area, cell number and cell size for experiments in (B) and (C). n = 30 for WT versus WT; n = 21 for WT versus *Tsc1.* Error bars represent ±SEM. ***p < 0.001.

Figure S6 shows additional characterization of the effects of QF, GAL4, or QF+GAL4 expression on imaginal disc differentiation.

UAS-Inverse Repeat transgenes as repressors against two fluorescent proteins and places these transgenes on the same chromosome arm in *trans* such that the FLP/FRT-mediated mitotic recombination creates two sibling cells, each losing one of the *RNAi* repressor genes (Yu et al., 2009). "Twin-spot generator" (TSG), which is analogous to the MADM method in mice (Zong et al., 2005), places two chimeric fluorescent proteins on the same chromosome arm in *trans.* Upon FLP/FRT-mediated recombination, two fluorescent proteins are reconstituted and can be segregated to daughter cells (Griffin et al., 2009). The potential advantage of the TSG method is the ability to examine clones shortly after induction since there is no perdurance of a repressor; however, marker expression is low because of the lack of binary system-based amplification. In addition, both markers are driven by a ubiquitous promoter, thereby limiting the utility for tracking lineages in complex tissues such as the nervous system as a result of frequent interference by a large number of background mitotic clones. Twin-spot MARCM uses fewer transgenes than coupled MARCM. However, both progeny are labeled by the same *GAL4* driver, thereby limiting the power for resolving cell division patterns (for example, siblings of a particular neuron may not be labeled by the same *GAL4* line) and lacking the flexibility for selective manipulation of different siblings. Coupled MARCM offers robust marker expression and versatility as it can combine all available *GAL4* and *QF* lines, whether cell-type-specific or ubiquitous. The combined use of ubiquitous *tubP-GAL4* and PN-specific *GH146-QF* was key to resolving cell division patterns in the PN lineage, and it could not have been achieved with TSG or twin-spot MARCM. Furthermore, coupled MARCM can be used for independent gain- and loss-of-function genetic manipulations of both progeny. An example is illustrated in the next section.

Analyzing Cell Proliferation and Growth with Coupled MARCM

Coupled MARCM allows direct comparison of two cell populations that arise from a single cell division within the same animal. Here, we illustrate its use to study cell proliferation and growth in the wing imaginal disc (Figure 5A).

The ~50,000 epithelial cells of the wing disc are produced by exponential cell division from less than 40 progenitor cells during the larval stages of *Drosophila* development (Bryant and Simpson, 1984). Clonal analysis in the wing imaginal disc is a sensitive strategy for studying the effects of genetic perturbations on cell growth or proliferation. To verify that QF expression does not affect normal cell growth or proliferation, we used coupled MARCM to label wild-type clones in the larval wing imaginal disc (Figure 5B). Clones were induced by heat shock at 48 hr after egg laying and examined 72 hr later. The area of the GAL4- and QF-labeled clones, their cell number, and cell size (Figures 5D, 5E, and 5F, respectively) were indistinguishable from one another. These results indicate that G-MARCM and Q-MARCM do not differentially affect cell proliferation or growth of wing disc cells. Additional control experiments indicated that high levels of QF expression did not interfere with growth and patterning of imaginal discs and the corresponding adult structures (Figure S6).

To show the utility of coupled MARCM in mutant analysis, we generated wing imaginal disc clones in which control cells were labeled by GAL4 and *Tuberous Sclerosis 1* (*Tsc1*) homozygous mutant cells were labeled by QF. Tsc1, along with its partner Tuberous Sclerosis 2 (Tsc2), forms a complex that negatively regulates the Tor pathway to affect both cell size and cell proliferation (Ito and Rubin, 1999; Potter et al., 2001; Tapon et al., 2001). We found that *Tsc1* mutant clones (labeled red via QF) were significantly larger than wild-type clones (labeled green

via GAL4) (Figure 5C), covering on average 2.9-fold larger area than their control sister clones (Figure 5D). To determine whether the increase in clone area is due to an increase in cell proliferation or cell size, we counted the number of cells within these labeled clones. We found a 2-fold increase in cell numbers in *Tsc1* mutant clones compared to the sister clones, yet only a 26% increase in cell size (Figures 5E and 5F), suggesting that mutation of *Tsc1* in rapidly dividing cells primarily leads to an increase in proliferative capacity. This example, although largely confirmatory of previous findings, illustrates the utility of coupled MARCM for investigating gene function in developmental processes.

Refining Transgene Expression by Intersecting GAL4 and QF Expression Patterns

A major power of the GAL4/UAS system is its ability to manipulate many cell types through thousands of GAL4 lines generated by enhancer trapping or GAL4 driven from specific promoters. Despite the abundance of GAL4 lines, their expression patterns are often too broad to establish the causality between the expression of a transgene in a particular cell type and a phenotype, especially if the phenotype is assayed at the organismal level. Combining GAL4- and QF-based binary systems into logic gates can create new expression patterns (Figure S7). Below we provide proof-of-principle examples for some of these strategies (Figure 6).

QF NOT GAL4

Like the previously characterized *GH146-GAL4* (Jefferis et al., 2001), *GH146-QF* is expressed in PNs that are derived from the anterodorsal, lateral and ventral neuroblast lineages (Figure 2B). The POU transcription factor Acj6 is expressed only in anterodorsal but not in lateral or ventral GH146-positive PNs (Komiyama et al., 2003). Acj6, and *acj6-GAL4*, an enhancer trap line inserted into the *acj6* locus, are also expressed in some GH146-negative anterodorsal PNs, in many olfactory receptor neurons (ORNs), in atypical PNs, and in lateral horn output neurons (Clyne et al., 1999; Komiyama et al., 2003; Suster et al., 2003; Komiyama et al., 2004; Jefferis et al., 2007; Lai et al., 2008). As shown in Figure 6A, when *GH146-QF* and *acj6-GAL4* are present in the same fly, and are detected via *QUAS-mtdT-HA* and *UAS-mCD8-GFP*, respectively, a large subset of anterodorsal PNs is labeled by both mCD8-GFP and mtdT-HA, whereas lateral and ventral PNs express mtdT-HA but not mCD8-GFP.

By introducing a *UAS-QS* transgene, we subtracted the GAL4-expressing cells from the QF-expressing cells such that the *QUAS-mtdT-HA* reporter was only expressed in the lateral and ventral, but not the anterodorsal, PNs (Figure 6B; compare Figure 6B_3 with Figure 6A_3). In this manner, we created "QF *NOT* GAL4," a new QF-dependent expression pattern. Using this logic gate, we observed nonoverlapping glomeruli labeled by Acj6-expressing anterodorsal PNs in green and QF-expressing lateral PNs in red (Figure 6B_2). This observation confirms directly in the same animal a previous finding that PNs from the anterodorsal and lateral lineages project dendrites to complementary and nonoverlapping glomeruli in the antennal lobe (Jefferis et al., 2001).

Expression pattern subtraction can also be visualized at the level of axon terminals. Both anterodorsal and lateral PNs project their axonal collaterals into the mushroom body calyx, where they terminate in large presynaptic boutons. In the absence of the *UAS-QS* transgene, these individual terminal boutons are labeled green, yellow, and red, representing axon terminals of PNs that are Acj6+/GH146- anterodorsal PNs, Acj6+/GH146+ anterodorsal PNs, and GH146+/Acj6- lateral PNs, respectively (Figure 6A_4). In the presence of *UAS-QS*, yellow terminal boutons are no longer present (Figure 6B_4), indicating that the cells labeled by *acj6-GAL4* have been subtracted from the *GH146-QF* expression pattern. This experiment allows a direct comparison of axon terminal distributions of anterodorsal and lateral PNs coinnervating the same mushroom body.

QF AND GAL4

By introducing two additional transgenes, *QUAS-FLP*, *UAS > stop > effector* (Figures 6C_1 and 6D_1; ">" represents FRT), or *UAS-FLP*, *QUAS > stop > effector* (Figure 6E_1), into an animal containing a *GAL4* and a *QF* line, only cells that express both QF and GAL4 ("QF *AND* GAL4") can be selectively visualized and genetically manipulated. Below we show three examples.

First, we studied the intersection of *GH146-QF* and *acj6-GAL4*. With the introduction of *UAS-FLP* and *QUAS > stop > mCD8-GFP*, anterodorsal PNs that are both Acj6+ and GH146+ were labeled (Figure 6C), as confirmed by the glomerular identity of dendritic projections of these neurons (data not shown). A previously described Acj6/GH146 double-positive cell from a separate lineage (Komiyama et al., 2003) was also labeled (Figure 6C_4, arrowhead). All other lateral and all ventral GH146+ PNs, which do not express Acj6, no longer expressed the marker. The marker was also not expressed in ORNs or lateral horn neurons, which express Acj6 but not GH146. Thus, we can express transgenes only in cells that express both GH146 and Acj6: a subset of anterodorsal PNs.

In the second and third examples, we studied the intersection between *GH146-QF* and *NP21-GAL4* using two *AND* gate strategies. *NP21-GAL4* is an enhancer trap line inserted near the promoter of *fruitless* (*fru*) (Hayashi et al., 2002) that drives the expression of the male-specific isoform of Fru (Fru^M), which is essential for regulating mating behavior (Demir and Dickson, 2005; Manoli et al., 2005). *NP21-GAL4* labels many neurons in the brain (Kimura et al., 2005) (Figure 6D_2), including PNs that project dendrites to the DA1 glomerulus (Figure 6E_2). In our first strategy (Figure 6D_1), we used *UAS-FLP* and *QUAS > stop > mCD8-GFP* and found that approximately ten PNs that innervated several glomeruli were selectively labeled (Figures 6D_3 and 6D_4). In our second strategy (Figure 6E_1), we used *QUAS-FLP* and *UAS > stop > mCD8-GFP* and found that the labeled PNs were restricted to only approximately five cells that project their dendrites to the DA1 glomerulus (Figures 6E_3 and 6E_4). The difference between these two strategies reflects the fact that in these intersectional strategies, the binary system used to drive FLP reports the cumulative developmental history, rather than only the adult expression, of the driver. Our data suggest that *NP21-GAL4* (and by inference fru^M) is expressed in more PN classes during development than in the adult. In both cases, the complex *NP21-GAL4* expression pattern outside of PNs has been reduced to very few cells. The comparison of expression patterns from the two strategies can pinpoint the cells that are at the intersection of *GH146-QF* and *NP21-GAL4* adult expression patterns. Future use of a perturbing effector could

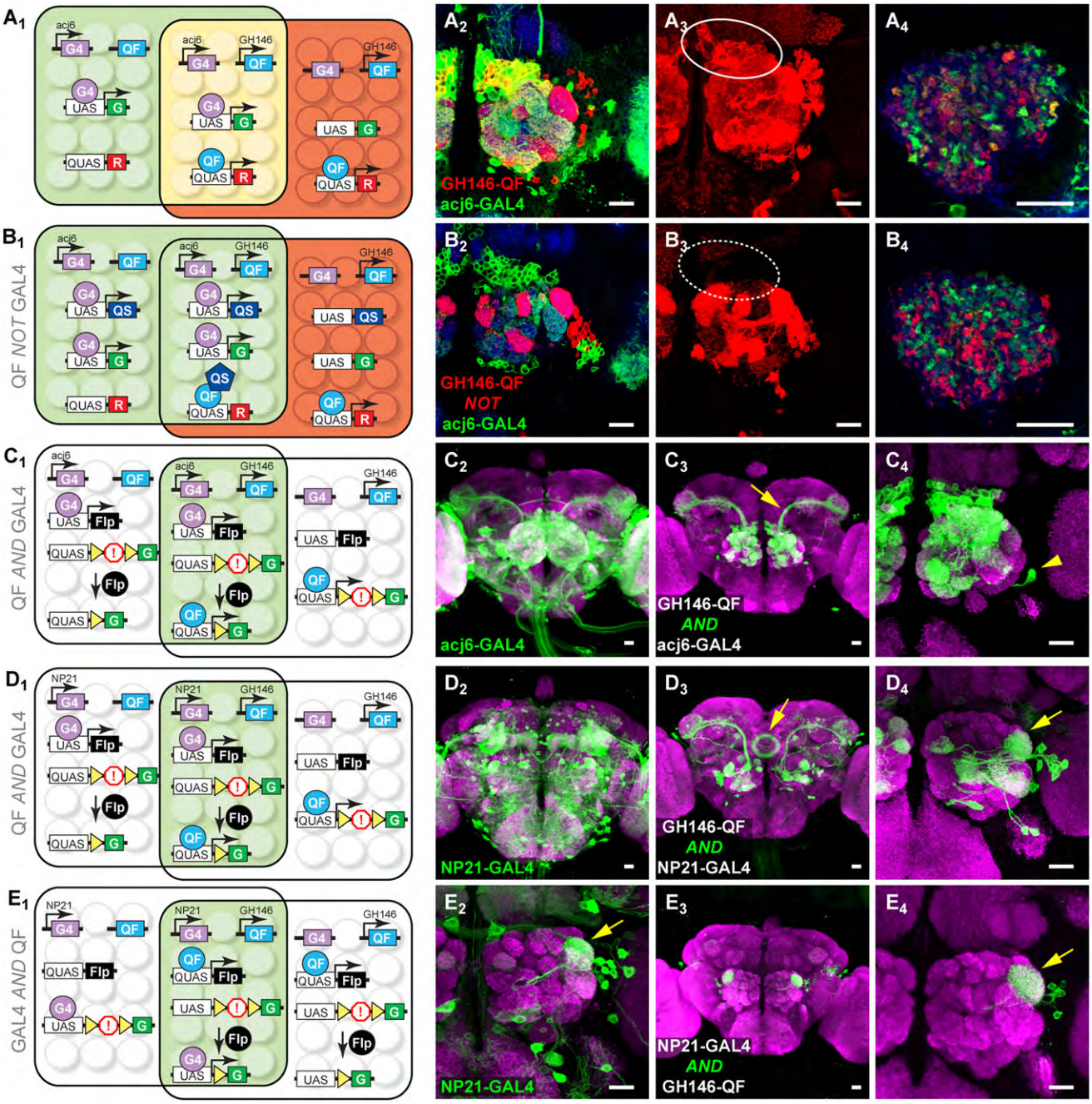

Figure 6. Intersectional Methods to Refine Transgene Expression

(A_1) Schematic showing two partially overlapping cell populations: one expressing an *acj6-GAL4*-driven green marker (within the left rectangle) and the other expressing a *GH146-QF*-driven red marker (within the right rectangle). Cells in the center express both GAL4 and QF and appear yellow.

(A_2–A_4) Single confocal sections (A_2 and A_4) or a Z projection (A_3) of the adult antennal lobe (A_2 and A_3) or mushroom body calyx (A_4) from flies with the genotype shown in (A_1). Green, red, and yellow cells in (A_2) represent PNs that express *acj6-GAL4* only, *GH146-QF* only, or both, respectively. Their dendrites form green, yellow, and red glomeruli (A_2). Their axons form green, red, and yellow terminal boutons in the mushroom body (A_4). (A_3) is the Z projection of the red channel for (A_2); the oval highlights cell bodies of anterodorsal PNs. Green, anti-CD8 staining for *UAS-mCD8-GFP*; red, anti-HA staining for *QUAS-mtdT-HA*; blue, neuropil marker.

(B_1) Schematic for "QF *NOT* GAL4" for *acj6-GAL4* and *GH146-QF*. *UAS-QS* is added to (A_1), resulting in the repression of QF activity in cells that express both QF and GAL4 (center). QF reporter expression is thus subtracted from the overlapping population of cells.

(B_2–B_4) Equivalent samples as (A_2)–(A_4), except with *UAS-QS* added. Compared to (A_3), anterodorsal PNs no longer express *QUAS-mtdT-HA* (dotted oval in B_3). There are no yellow cells and glomeruli in the antennal lobe (B_2), or yellow terminal boutons in the mushroom body (B_4).

(A and B) Note that in the experiments shown, for clear visualization of only non-ORN processes in the antennal lobe, antennae and maxillary palps were removed 10 days prior to staining, causing all Acj6-expressing ORN axons to degenerate.

lead to functional characterization of this small genetically defined group of cells.

Comparisons with Other Methods

An *AND* gate can be achieved by utilizing the split-GAL4 system (Luan et al., 2006). The benefit of our method is that it can take advantage of the thousands of available and well-characterized GAL4 lines, whereas the split-GAL4 system needs to generate new split N-GAL4 and C-GAL4 lines. In addition, reconstituted GAL4 from the split GAL4 system is not as strong as wild-type GAL4 in driving transgene expression (Luan et al., 2006).

The intersection between FLP/FRT and GAL4/UAS can also be used directly as an *AND* gate without going through a second binary system to express FLP (Stockinger et al., 2005; Hong et al., 2009). Both this method and our method have the caveats of transient FLP expression during development, as well as the possibility that FLP/FRT-mediated recombination may not occur in all cells that express FLP. Although our method requires one additional transgene, it offers several advantages over promoter-driven FLP. First, our method does not require the generation of separate tissue or cell type-specific FLP lines. Second, by inducing higher FLP levels due to transcriptional amplification of binary expression, our method should more readily overcome problems of incomplete recombination. Indeed, counts of the number of DA1-projecting PNs that are part of the *NP21-GAL4* expression pattern with or without the *AND* gate with *GH146-QF* are similar (*NP21-GAL4*: 5.2 ± 0.1, n = 48; *GH146-QF/QUAS-FLP AND NP21-GAL4*: 5.1 ± 0.1, n = 10), suggesting nearly complete FLP/FRT mediated recombination. Third, our method offers two complementary *AND* gate strategies, which together can be used to overcome the ambiguities arising from transient developmental expression. Fourth, transient developmental expression mediated by *QUAS-FLP* could in principle be suppressed by introduction of *tubP-QS*, and the suppression could be reversed by supplying the flies with quinic acid at appropriate developmental stages.

The "QF *NOT* GAL4" or "GAL4 *NOT* QF" (Figure S7) strategies are conceptually similar to GAL80 subtraction of GAL4 expression (Lee and Luo, 1999). If one were to generate a large number of GAL80 enhancer trap or promoter driven lines, one could use this set to subtract their expression patterns from GAL4 expression patterns. One limitation of this approach is that the GAL80 expression pattern is difficult to determine at high resolution because it is based on suppression of GAL4-induced gene expression. In addition, GAL80 levels must be sufficiently high to ensure proper suppression of GAL4, which may not be true for many enhancer trap or promoter-driven GAL80 transgenes. By contrast, the *NOT* gate we describe here utilizes the expression patterns of two transcription factors, which express the appropriate repressor through binary amplification, and should therefore circumvent both limitations above.

A major limitation of our intersectional strategies for refinement of gene expression is the availability of QF drivers with different expression patterns. So far, we were unsuccessful in generating *tubP-QF* transgenic animals, suggesting that QF is toxic to flies when highly expressed in a ubiquitous manner or in a particular developmental stage or tissue (see the Extended Experimental Procedures). Nonetheless, we isolated many QF enhancer traps that express strongly in imaginal discs, epithelial tissues, glia, and neurons (Figures S2B and S3). We hope that our proof-of-principle examples here will stimulate the *Drosophila* community to generate large numbers of enhancer trap and promoter-driven QF lines in the future. The number of new expression patterns created by intersections between GAL4 and QF should be multiplicative. For instance, 100 QF lines in combination with 10,000 GAL4 lines, given sufficient expression overlap and utilizing different logic gates (Figure S7), should in principle generate millions of new effector expression patterns.

Defining PNs Responsible for Olfactory Attraction

By expressing an effector that alters neuronal activity, intersectional approaches can be used to dissect the function of neuronal circuits. We used this approach to assay the function of PNs in an olfactory attraction behavior. Instead of expressing a marker in specific populations of neurons, we expressed *shibire^{ts1}* (*shi^{ts}*), a temperature-sensitive variant of the protein dynamin that dominantly interferes with synaptic vesicle recycling

(C_1) Schematic for "QF *AND* GAL4" for *acj6-GAL4* and *GH146-QF*. GAL4 driven FLP results in the removal of a transcriptional stop (!) from a *QUAS* reporter (within the left rectangle), but the reporter can only be expressed in cells where QF is expressed (within the right rectangle). Thus, only the cells in the overlap (center) express the reporter.

(C_2) Confocal stack of a whole mount central brain showing reporter (mCD8-GFP) expression driven by *acj6-GAL4*, which labels many types of neurons including most ORNs, olfactory PNs and optic lobe neurons.

(C_3 and C_4) The *AND* gate between *GH146-QF* and *acj6-GAL4* (genotype as in C_1) limits mCD8-GFP expression to a cluster of anterodorsal PNs and a single lateral neuron (arrowhead in C_4). Arrow in (C_3), axons of anterodorsal PNs.

(D_1) Schematic for "QF *AND* GAL4" similar to (C_1), but for *NP21-GAL4* and *GH146-QF*.

(D_2) Confocal stack of whole-mount central brain showing reporter (mCD8-GFP) expression driven by *NP21-GAL4*.

(D_3 and D_4) The *AND* gate between *GH146-QF* and *NP21-GAL4* limits reporter expression to a few classes of PNs that project to several glomeruli including DA1 (arrow in D_4) and to neurons that project to the ellipsoid body (arrow in D_3).

(E_1) Schematic for an alternative approach to "GAL4 *AND* QF" for *NP21-GAL4* and *GH146-QF*. Here, FLP is driven by QF, and the reporter is driven by GAL4.

(E_2) High magnification of the *NP21-GAL4* expression pattern centered at the antennal lobe. In the adult, only one class of lateral PNs projecting to the DA1 glomerulus (arrow) is evident.

(E_3 and E_4) This *AND* gate between *GH146-QF* and *NP21-GAL4* limits expression to a single class of lateral PNs that project to the DA1 glomerulus (arrow in E_4). Occasional expression is also found in a few cells in the anterior lateral region of the brain.

Genotypes: *acj6-GAL4, GH146-QF, UAS-mCD8-GFP, QUAS-mtdT-HA* (A), *acj6-GAL4, GH146-QF, UAS-mCD8-GFP, QUAS-mtdT-HA, UAS-QS* (B), *acj6-GAL4, UAS-mCD8-GFP* (C_2), *acj6-GAL4, GH146-QF, UAS-FLP, QUAS > stop > mCD8-GFP* (C_3 and C_4), *NP21-GAL4, UAS-mCD8-GFP* (D_2 and E_2), *NP21-GAL4, GH146-QF, UAS-FLP, QUAS > stop > mCD8-GFP* (D_3 and D_4), *NP21-GAL4, GH146-QF, UAS > stop > mCD8-GFP, QUAS-FLP* (E_3 and E_4). Yellow triangle or ">," FRT site; "!" or "stop," transcriptional stop. Scale bars represent 20 μm. Figure S7 shows strategies to generate 12 QF and GAL4 intersectional logic gates.

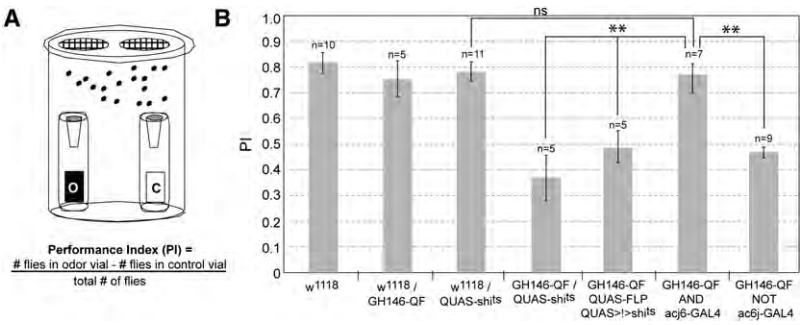

Figure 7. Defining PNs Responsible for Olfactory Attraction with Intersectional Methods

(A) Schematic of the olfactory trap assay. O, 1% ethyl acetate in mineral oil; C, control (mineral oil alone). A performance index (PI) is used to measure olfactory attraction.

(B) Performance index plots of flies of listed genotypes. Error bars represent ±SEM. **p ≤ 0.01. ns, not significant. Genotypes: GH146-QF *AND* acj6-GAL4: *acj6-GAL4*, *GH146-QF*, *UAS-FLP*, *QUAS > stop > shibire^{ts1}*; GH146-QF *NOT* acj6-GAL4: *acj6-GAL4*, *GH146-QF*, *UAS-QS*, *QUAS-shibire^{ts1}*. ">," FRT site; "!" or "stop," transcriptional stop.

(Kitamoto, 2001). At the nonpermissive temperature, synaptic transmission of neurons that express *shi^{ts}* is reversibly inhibited. This approach allowed us to selectively inhibit different populations of PNs—lateral and ventral (GH146-QF *NOT* acj6-GAL4; Figure 6B) or anterodorsal (GH146-QF *AND* acj6-GAL4; Figure 6C)—and then assay behavioral attraction to the fruity odorant ethyl acetate using a modified trap assay (Larsson et al., 2004) (Figure 7). Similar to controls, flies containing only *GH146-QF* or *QUAS-shi^{ts}* exhibited strong attraction to ethyl acetate. When all GH146+ PNs were inhibited (*GH146-QF+QUAS-shi^{ts}* or *GH146-QF+QUAS-FLP+QUAS > stop > shi^{ts}*), there was a significant deficit in olfactory attraction. However, when only anterodorsal GH146+ PNs were inhibited, attraction remained normal. In contrast, when lateral/ventral GH146+ PNs were inhibited, there was a deficit in olfactory attraction akin to the inhibition of all GH146+ PNs. These results suggest that, in this behavioral context, attraction to ethyl acetate is mediated by the lateral/ventral, and not anterodorsal, subpopulations of PNs.

Conclusions and Perspectives

In conclusion, we demonstrate that the Q repressible binary expression system functions well outside its native *Neurospora*, from cultured *Drosophila* and mammalian cells to *Drosophila* in vivo. We have generated and validated a substantial number of tools (Table S1, Figures S2 and S3) that can be used for many applications, as illustrated by the examples given above. Below, we discuss a few future developments and applications.

Genetic Dissection of Neural Circuits

Drosophila has emerged as an attractive model system to establish causal links between the functions of individual classes of neurons, information processing within neural circuits, and animal behavior. A bottleneck in this endeavor is the genetic access to specific populations of neurons with reproducible precision, such that one can label them with markers for anatomical analysis, express genetically encoded indicators to record their activity, and silence or activate these neurons to examine the consequences to circuit output or to animal behavior (Luo et al., 2008). The intersectional methods we describe should greatly increase the precision of genetic access to specific neuronal populations, especially as more QF drivers are characterized.

High-Resolution Mosaic Analysis

Although MARCM is a powerful tool for identification and functional studies of genes that act cell autonomously, it is less adaptable to studies of genes that act non-cell autonomously. The ability to perform MARCM analysis independently from GAL4/UAS should expand the power of mosaic analysis for genes that function in intercellular communication. For example, using GAL4/UAS, one can perturb the function of a group of cells, while using Q-MARCM to examine the consequences of the perturbation on a small subset of interacting cells. Furthermore, both systems can be used in the same animal for independent perturbations of two populations of interacting cells, via both loss- and gain-of-function approaches. Finally, these approaches can be expanded into genetic screens where, for example, the GAL4 binary system is used to drive an RNAi library in a large group of cells while the Q system is used to label a small population of neurons with high resolution.

Beyond the Nervous System and Drosophila

The Q system should be widely applicable beyond the *Drosophila* nervous system. We have provided an example of clonal phenotypic analysis in the wing disc for cell growth and proliferation. Similar studies could be used for the identification and characterization of tumor suppressors or oncogenes that function cell autonomously or non-cell autonomously. The Q system should in principle permit transgene expression, lineage and mosaic analysis in many other *Drosophila* tissues. Finally, QF/QUAS-induced transgene expression is ~30-fold more effective in mammalian cells compared with GAL4/UAS. This fact may make the Q binary expression system more effective than GAL4/UAS for transgene expression in mice (Ornitz et al., 1991; Rowitch et al., 1999). Indeed, the Q system could be extended to all organisms conducive to transgenesis.

EXPERIMENTAL PROCEDURES

QF and QS cDNAs were obtained by PCR with a cosmid, pLorist-HO35F3 from the Fungal Genetics Stock Center, as the template. QUAS was constructed with five copies of naturally occurring QF binding sites (each 16 bp long, shown in capital letters, with spacer sequences in small letters): GGGTAATCGCT TATCCTcGGATAAACAATTATCCtcacGGGTAATCGCTTATCCgctcGGGTAAT CGCTTATCCtcGGGTAATCGCTTATCCtt.

See the Extended Experimental Procedures for details on the construction of plasmids and transgenic flies, cell transfection, *Drosophila* genetics, mosaic analysis, imaging, and behavior.

All plasmids and sequence files have been deposited to Addgene. Most fly stocks in Table S1 have been deposited to the Bloomington Stock Center. Other fly stocks are available upon request.

ACCESSION NUMBERS

Sequences for representative QF, QS, and QUAS plasmid constructs were deposited to GenBank and have the following accession numbers:

pattB-QF-hsp70, #HM068614; pBS-SK-QS, #HM068612; and pQUAST, #HM068613.

SUPPLEMENTAL INFORMATION

Supplemental Information includes Extended Experimental Procedures, seven figures, and one table and can be found with this article online at doi:10.1016/j.cell.2010.02.025.

ACKNOWLEDGMENTS

We thank D. Luginbuhl, M. Tynan La Fontaine, and T. Chou for technical assistance; K. Wehner for HeLa cells and mouse anti-HA and mouse anti-fibrillarin antibodies; M. Simon for S2 cells and adult eye sectioning; T. Clandinin for 24B10 antibodies; S. Block for luminometer usage; the Fungal Genetics Stock Center for cosmids containing QF and QS; the Developmental Biology Hybridoma Bank for monoclonal antibodies; the Bloomington Stock Center for flies; and D. Berdnik, Y.-H. Chou, K. Miyamichi, M. Spletter, L. Sweeney, and W. Hong for comments on the manuscript. This research was supported by grants from the National Institutes of Health and Human Frontiers Science Program. C.J.P. and B.T. were supported by the Damon Runyon Cancer Research Foundation (C.J.P., DRG-1766-03; B.T., DRG-1819-04). L. Liang was supported by the Stanford Graduate Fellowship. L. Luo is an investigator of the Howard Hughes Medical Institute. C.J.P. performed all the *Drosophila* in vivo experiments, with the help of E.V.R. B.T. identified the *qa* system from *Neurospora* as a candidate binary expression system and performed the *Drosophila* and mammalian cultured cell experiments. L. Liang performed the quantitative analysis in Figure 5. L. Luo supervised the project, and wrote the paper with C.J.P. and B.T.

Received: August 4, 2009
Revised: January 7, 2010
Accepted: February 16, 2010
Published: April 29, 2010

REFERENCES

Baum, J.A., Geever, R., and Giles, N.H. (1987). Expression of qa-1F activator protein: identification of upstream binding sites in the qa gene cluster and localization of the DNA-binding domain. Mol. Cell. Biol. *7*, 1256–1266.

Berdnik, D., Fan, A.P., Potter, C.J., and Luo, L. (2008). MicroRNA processing pathway regulates olfactory neuron morphogenesis. Curr. Biol. *18*, 1754–1759.

Brand, A.H., and Perrimon, N. (1993). Targeted gene expression as a means of altering cell fates and generating dominant phenotypes. Development *118*, 401–415.

Bryant, P.J., and Simpson, P. (1984). Intrinsic and extrinsic control of growth in developing organs. Q. Rev. Biol. *59*, 387–415.

Clyne, P.J., Certel, S.J., de Bruyne, M., Zaslavsky, L., Johnson, W.A., and Carlson, J.R. (1999). The odor specificities of a subset of olfactory receptor neurons are governed by Acj6, a POU-domain transcription factor. Neuron *22*, 339–347.

Demir, E., and Dickson, B.J. (2005). fruitless splicing specifies male courtship behavior in Drosophila. Cell *121*, 785–794.

Dietzl, G., Chen, D., Schnorrer, F., Su, K.C., Barinova, Y., Fellner, M., Gasser, B., Kinsey, K., Oppel, S., Scheiblauer, S., et al. (2007). A genome-wide transgenic RNAi library for conditional gene inactivation in Drosophila. Nature *448*, 151–156.

Fischer, J.A., Giniger, E., Maniatis, T., and Ptashne, M. (1988). GAL4 activates transcription in Drosophila. Nature *332*, 853–856.

Giles, N.H., Geever, R.F., Asch, D.K., Avalos, J., and Case, M.E. (1991). The Wilhelmine E. Key 1989 invitational lecture. Organization and regulation of the qa (quinic acid) genes in Neurospora crassa and other fungi. J. Hered. *82*, 1–7.

Golic, K.G., and Lindquist, S. (1989). The FLP recombinase of yeast catalyzes site-specific recombination in the Drosophila genome. Cell *59*, 499–509.

Gossen, M., and Bujard, H. (1992). Tight control of gene expression in mammalian cells by tetracycline-responsive promoters. Proc. Natl. Acad. Sci. USA *89*, 5547–5551.

Griffin, R., Sustar, A., Bonvin, M., Binari, R., del Valle Rodriguez, A., Hohl, A.M., Bateman, J.R., Villalta, C., Heffern, E., Grunwald, D., et al. (2009). The twin spot generator for differential Drosophila lineage analysis. Nat. Methods *6*, 600–602.

Hayashi, S., Ito, K., Sado, Y., Taniguchi, M., Akimoto, A., Takeuchi, H., Aigaki, T., Matsuzaki, F., Nakagoshi, H., Tanimura, T., et al. (2002). GETDB, a database compiling expression patterns and molecular locations of a collection of Gal4 enhancer traps. Genesis *34*, 58–61.

Hong, W., Zhu, H., Potter, C.J., Barsh, G., Kurusu, M., Zinn, K., and Luo, L. (2009). Leucine-rich repeat transmembrane proteins instruct discrete dendrite targeting in an olfactory map. Nat. Neurosci. *12*, 1542–1550.

Huiet, L., and Giles, N.H. (1986). The qa repressor gene of Neurospora crassa: wild-type and mutant nucleotide sequences. Proc. Natl. Acad. Sci. USA *83*, 3381–3385.

Ito, N., and Rubin, G.M. (1999). gigas, a Drosophila homolog of tuberous sclerosis gene product-2, regulates the cell cycle. Cell *96*, 529–539.

Jefferis, G.S.X.E., Marin, E.C., Stocker, R.F., and Luo, L. (2001). Target neuron prespecification in the olfactory map of Drosophila. Nature *414*, 204–208.

Jefferis, G.S., Potter, C.J., Chan, A.M., Marin, E.C., Rohlfing, T., Maurer, C.R., Jr., and Luo, L. (2007). Comprehensive maps of Drosophila higher olfactory centers: spatially segregated fruit and pheromone representation. Cell *128*, 1187–1203.

Kimura, K., Ote, M., Tazawa, T., and Yamamoto, D. (2005). Fruitless specifies sexually dimorphic neural circuitry in the Drosophila brain. Nature *438*, 229–233.

Kitamoto, T. (2001). Conditional modification of behavior in Drosophila by targeted expression of a temperature-sensitive shibire allele in defined neurons. J. Neurobiol. *47*, 81–92.

Komiyama, T., Johnson, W.A., Luo, L., and Jefferis, G.S. (2003). From lineage to wiring specificity. POU domain transcription factors control precise connections of Drosophila olfactory projection neurons. Cell *112*, 157–167.

Komiyama, T., Carlson, J.R., and Luo, L. (2004). Olfactory receptor neuron axon targeting: intrinsic transcriptional control and hierarchical interactions. Nat. Neurosci. *7*, 819–825.

Lai, S.L., and Lee, T. (2006). Genetic mosaic with dual binary transcriptional systems in Drosophila. Nat. Neurosci. *9*, 703–709.

Lai, S.L., Awasaki, T., Ito, K., and Lee, T. (2008). Clonal analysis of Drosophila antennal lobe neurons: diverse neuronal architectures in the lateral neuroblast lineage. Development *135*, 2883–2893.

Larsson, M.C., Domingos, A.I., Jones, W.D., Chiappe, M.E., Amrein, H., and Vosshall, L.B. (2004). Or83b encodes a broadly expressed odorant receptor essential for Drosophila olfaction. Neuron *43*, 703–714.

Lee, T., and Luo, L. (1999). Mosaic analysis with a repressible cell marker for studies of gene function in neuronal morphogenesis. Neuron *22*, 451–461.

Lee, T., Lee, A., and Luo, L. (1999). Development of the Drosophila mushroom bodies: sequential generation of three distinct types of neurons from a neuroblast. Development *126*, 4065–4076.

Lin, S., Lai, S.L., Yu, H.H., Chihara, T., Luo, L., and Lee, T. (2010). Lineage-specific effects of Notch/Numb signaling in post-embryonic development of the Drosophila brain. Development *137*, 43–51.

Luan, H., Peabody, N.C., Vinson, C.R., and White, B.H. (2006). Refined spatial manipulation of neuronal function by combinatorial restriction of transgene expression. Neuron *52*, 425–436.

Luo, L. (2007). Fly MARCM and mouse MADM: genetic methods of labeling and manipulating single neurons. Brain Res. Brain Res. Rev. *55*, 220–227.

Luo, L., Callaway, E.M., and Svoboda, K. (2008). Genetic dissection of neural circuits. Neuron *57*, 634–660.

Manoli, D.S., Foss, M., Villella, A., Taylor, B.J., Hall, J.C., and Baker, B.S. (2005). Male-specific fruitless specifies the neural substrates of Drosophila courtship behaviour. Nature *436*, 395–400.

Marin, E.C., Jefferis, G.S.X.E., Komiyama, T., Zhu, H., and Luo, L. (2002). Representation of the glomerular olfactory map in the Drosophila brain. Cell *109*, 243–255.

Marin, E.C., Watts, R.J., Tanaka, N.K., Ito, K., and Luo, L. (2005). Developmentally programmed remodeling of the Drosophila olfactory circuit. Development *132*, 725–737.

McGuire, S.E., Le, P.T., Osborn, A.J., Matsumoto, K., and Davis, R.L. (2003). Spatiotemporal rescue of memory dysfunction in Drosophila. Science *302*, 1765–1768.

Nollet, L.M.L. (2000). Food Analysis by HLPC, Second Edition (New York: CRC Press).

Nordlander, R.H., and Edwards, J.S. (1969). Postembryonic brain development in the monarch butterfly, Danaus plexippus pleisippus, L. I. cellular events during brain morphogenesis. Wilhelm Roux' Archiv *162*, 197–217.

Ornitz, D.M., Moreadith, R.W., and Leder, P. (1991). Binary system for regulating transgene expression in mice: targeting int-2 gene expression with yeast GAL4/UAS control elements. Proc. Natl. Acad. Sci. USA *88*, 698–702.

Patel, V.B., Schweizer, M., Dykstra, C.C., Kushner, S.R., and Giles, N.H. (1981). Genetic organization and transcriptional regulation in the qa gene cluster of Neurospora crassa. Proc. Natl. Acad. Sci. USA *78*, 5783–5787.

Pfeiffer, B.D., Jenett, A., Hammonds, A.S., Ngo, T.T., Misra, S., Murphy, C., Scully, A., Carlson, J.W., Wan, K.H., Laverty, T.R., et al. (2008). Tools for neuroanatomy and neurogenetics in Drosophila. Proc. Natl. Acad. Sci. USA *105*, 9715–9720.

Potter, C.J., Huang, H., and Xu, T. (2001). Drosophila Tsc1 functions with Tsc2 to antagonize insulin signaling in regulating cell growth, cell proliferation, and organ size. Cell *105*, 357–368.

Rørth, P., Szabo, K., Bailey, A., Laverty, T., Rehm, J., Rubin, G.M., Weigmann, K., Milán, M., Benes, V., Ansorge, W., and Cohen, S.M. (1998). Systematic gain-of-function genetics in Drosophila. Development *125*, 1049–1057.

Rowitch, D.H., S-Jacques, B., Lee, S.M., Flax, J.D., Snyder, E.Y., and McMahon, A.P. (1999). Sonic hedgehog regulates proliferation and inhibits differentiation of CNS precursor cells. J. Neurosci. *19*, 8954–8965.

Stocker, R.F., Heimbeck, G., Gendre, N., and de Belle, J.S. (1997). Neuroblast ablation in Drosophila P[GAL4] lines reveals origins of olfactory interneurons. J. Neurobiol. *32*, 443–456.

Stockinger, P., Kvitsiani, D., Rotkopf, S., Tirián, L., and Dickson, B.J. (2005). Neural circuitry that governs Drosophila male courtship behavior. Cell *121*, 795–807.

Suster, M.L., Martin, J.R., Sung, C., and Robinow, S. (2003). Targeted expression of tetanus toxin reveals sets of neurons involved in larval locomotion in Drosophila. J. Neurobiol. *55*, 233–246.

Tapon, N., Ito, N., Dickson, B.J., Treisman, J.E., and Hariharan, I.K. (2001). The Drosophila tuberous sclerosis complex gene homologs restrict cell growth and cell proliferation. Cell *105*, 345–355.

Xu, T., and Rubin, G.M. (1993). Analysis of genetic mosaics in developing and adult Drosophila tissues. Development *117*, 1223–1237.

Yu, H.H., Chen, C.H., Shi, L., Huang, Y., and Lee, T. (2009). Twin-spot MARCM to reveal the developmental origin and identity of neurons. Nat. Neurosci. *12*, 947–953.

Zong, H., Espinosa, J.S., Su, H.H., Muzumdar, M.D., and Luo, L. (2005). Mosaic analysis with double markers in mice. Cell *121*, 479–492.

Cell

EXTENDED EXPERIMENTAL PROCEDURES

Recombinant DNA Construction

Plasmids were constructed by standard subcloning, synthesis and/or PCR. For PCR amplifications, we usually used Phusion Taq polymerase (Finnzymes, Catalog # F530L), and in a few cases Platinum Pfx polymerase (Invitrogen, Catalog # 11708-021). When synthetic oligos or PCR were involved in plasmid construction, the sequence of the construct was verified by DNA sequencing. Please note that four constructs described below (pattB-QF-SV40, pattB-QF-hsp70, pattB-DSCP-QF-SV40, pBS-SK-QS) were not used in the experiments described in this report but are included here as they simplify the generation of additional Q system reagents.

Three parent plasmids were used for a number of constructs below:

1) pP_{AC5C}-PL (gift of Rui Zhou, Harvard Medical School), which contains *Drosophila actin 5c* promoter and its polyadenylation sequence.
2) pCDNA3.1-myc-His-A (Invitrogen), which contains human cytomegalovirus (CMV) immediate-early promoter, myc and six-Histidine tags for C-terminal fusion, and bovine growth hormone polyadenylation signal sequence. All cDNAs that were cloned into this plasmid contained a stop codon preceding the Myc and His tags, thereby preventing the fusion of the cDNAs with the tags.
3) pBluescript SK (+) (Stratagene).

pQUAS-GG

This plasmid contains 5 copies of naturally occurring QF binding sites (each 16 bp long, shown in capital letters, with spacer sequences in small letters): GGGTAATCGCTTATCCtcGGATAAACAATTATCCtcacGGGTAATCGCTTATCCgctcGGGTAATCGCTTATCCtcGGGTAATCGCTTATCCtt

This sequence was assembled from overlapping primers and cloned using XhoI and HindIII into pBluescript containing hsp70 minimal promoter (Brand and Perrimon, 1993) and an optimized GFP split with an intron (GG) (Zong et al., 2005).

pQUAS-luc2

The XhoI/NcoI fragment containing QUAS-Pmin was subcloned from pQUAS-GG into pGL4.23 (Promega) to replace its minimal promoter. pGL4.23 contains synthetic firefly luciferase gene (luc2), which has been codon optimized for high expression in mammalian cells.

pAC-QF

QF cDNA was obtained by PCR using primers PR50 (aatggatcccaacatgccgcctaaacgcaagac) and PR51 (aatgcggccgcctattgctcatacgtgttgatatcg), and the cosmid, pLorist-HO35F3 from the Fungal Genetics Stock Center, as the template. The PCR fragment was cloned into pP_{AC5C}-PL using BamHI and NotI. The QF gene is intronless.

pCMV-QF

Obtained by subcloning QF cDNA using BamHI and Not I from pAC-QF into pCDNA3.1-myc-His-A (Invitrogen).

pCMV-QS

QS cDNA was obtained by PCR using primers PR53 (aatggtacccaacatgaacaccatcccggcac) and PR54 (aatgcggccgctcaagatatttgcgttgcaattc) using a cosmid, pLorist-HO35F3 from the Fungal Genetics Stock Center, as the template. The PCR fragment was initially cloned into pP_{AC5C}-PL using Acc65 I and NotI to obtain the QS gene containing a single intron. The intron was subsequently removed by creating two PCR products that were cloned using 3-way ligation into pCDNA3.1-Mys-His-A (Invitrogen) using Acc65I and NotI and blunt ends at the exon-exon junction. The primers used to create the first exon are: PR53 (see above) + PR190 (agagcctagaggtactctgtgggcgg); and the second exon are: PR58 (tggtcggcgcccaattcc) + PR54 (see above).

pAC-QS

Obtained by subcloning intronless QS from pCMV-QS using Acc65I and NotI into pP_{AC5C}-PL.

pUAS-GG

The BamHI/BglI fragment from pUAST (Brand and Perrimon, 1993), containing 5 copies of a GAL4 binding site and the *Drosophila* hsp70 minimal promoter was subcloned into BamHI site of pBluescript containing an optimized GFP split with an intron (GG) (Zong et al., 2005). This strategy generates a hybrid BglII/BamHI site in front of the GFP.

pUAS-luc2

Obtained by subcloning 5 copies of GAL4-binding UAS sequence and the hsp70 minimal promoter from pUAS-GG into pGL4.23 using HindIII and NcoI. The 5xUAS+Pmin fragment from pUAS-GG originates from pUAST (Brand and Perrimon, 1993).

pAC-GAL4 and pCMV-GAL4

GAL4 cDNA was PCR amplified using primers PR509 (CCCCGGATCCCAACatgaagctactgtcttctatcgaaca) and PR510 (CGGTTAACGCGGCCGCttactctttttttgggtttggtg), and a lab vector, pCA-GAL4 as the template. The PCR product was cloned using BamHI and NotI into pP_{AC5C}-PL and pCDNA3.1-myc-His-A, respectively.

pAC-GAL80 and pCMV-GAL80

GAL80 cDNA was PCR amplified using primers PR511 (CCCCGGATCCCAACatggactacaacaagagatcttcgg) and PR512 (CGGTTAACGCGGCCGCttataaactataatgcgagatattgctaacg), and a lab vector, pCA-GAL80 as the template. The PCR product was cloned using BamHI and NotI into pP_{AC5C}-PL and pCDNA3.1-myc-His-A, respectively.

pAC-hRluc

Synthetic Renilla luciferase that was codon optimized for expression in mammalian cells (hRluc) was amplified using primers PR444 (ataaGGTACCaaaATGGCTTCCAAGGTGTACGA) and PR443 (ataaGCGGCCGCTTACTGCTCGTTCTTCAGCA), and pGL4.75 (hRluc/CMV, Promega, catalog # E6931) as the template. The PCR product was cloned into pP_{AC5C}-PL using Acc65I and NotI.

pQUAST

This vector was designed to mimic the multi-cloning site of the pUAST vector (Brand and Perrimon, 1993) thereby allowing easy exchange of inserts between pUAST and pQUAST. pUAST was digest by SphI and EcoRI and blunted with Klenow to remove the 5xUAS and hsp70 minimal promoter (minP). pQUAS-GG was digested with BamHI and EcoRI to excise the 5xQUAS and Pmin and then blunted. The 5xQUAS-Pmin promoter was then ligated into the modified pUAST vector to generate pQUAST. Any gene X can be subcloned from pUAST-geneX into pQUAST using the same restriction sites that were originally utilized for pUAST-geneX construction. If the pUAST-geneX plasmid is not available, genomic DNA from flies containing the *UAS-geneX* transgene can be used. In this case, pQUAST-geneX can be constructed as follows:

1) PCR amplify the UAS insert from *UAS-geneX* genomic DNA by using the primer pairs genUASFOR (GCTTCGTCTACGGAGC GACAATTCAATTCAAAC) and genUASREVsv40 (GCAGTAGCCTCATCATCACTAGATGGCATTTCTTC). These primers will amplify the insert for any UAS construct, including the restriction sites used for cloning of that insert into the UAS vector.
2) If the restriction sites used for cloning of the UAS insert are unknown, sequence the PCR fragment using UASFOR-SEQ (TCAAACAAGCAAAGTGAACACG) and SV40REV-SEQ (CCATTCATCAGTTCCATAGGTTGG) primers.
3) Digest the PCR product with appropriate enzymes for cloning into pQUAST.

pQUAS-DSCP

pQUAST was digested with EcoRI, which removed the hsp70 minimal promoter. A PCR fragment containing the DSCP promoter was PCR amplified from pBPGUw (Pfeiffer et al., 2008) with 5′ EcoRI and 3′ MfeI site, and was ligated into pQUAST to generate pQUAS-DSCP. Expression levels between pQUAS-DSCP and pQUAST vectors have not been directly compared (for example, by having the reporter constructs integrated at the same attP location). Nonetheless, pQUAS-DSCP-FLPo and pQUAST-FLPo transgenic flies both showed strong FLP activity in the intersectional studies shown in Figure 6E.

pmCD8-GFP,y+

This enhancer trap vector is based on the pGalW vector (Gerlitz et al., 2002). The GAL4 insert from pGalW was removed by complete NotI and partial XbaI digestion and replaced with the GAL80 ORF isolated as a NotI/XbaI fragment from pCasper-tubP-GAL80 (Lee and Luo, 1999), to generate the plasmid pG80,w+. To generate pG80,y+, the white gene from pG80,w+ was excised by EcoRV/SacII digestion, the vector was blunted with Klenow, and replaced with the yellow gene as a blunted SalI fragment from the y S/G plasmid (a gift from Pamela Geyer, University of Iowa). To generate pmCD8-GFP,y+, the GAL80 insert was excised by NotI digestion and replaced with mCD8-GFP which was PCR amplified from pUAST-mCD8-GFP to include 5′ and 3′ NotI restriction sites (see also Berdnik et al., 2006).

pQUAST-mCD8-GFP

The NotI fragment containing CD8-GFP-SV40 from the enhancer trap construct pCD8-GFP,y+ was cloned into pQUAST.

ptubP-QS

The QS cDNA was excised from pAC-QS with Acc65I and NotI, blunted, and ligated into a blunted pCasper-tubulin-GAL80, from which the GAL80 insert was removed by digestion with NotI/XbaI.

pBac-GH146-QF

pBAC-3xPDsRed-GH146-MCS with FseI-AscI-AvrII multi-cloning site has been previously described (Hong et al., 2009). QF cDNA with 5′ FseI and 3′ AvrII restriction sites was amplified from pAC-QF by PCR, and cloned into the FseI/AvrII restriction sites of pBAC-GH146 to yield pBac-GH146-QF.

pQUAST-mtdT-3xHA, pUASTattB-mtdT-3xHA

The N-terminal membrane tag on tdTomato contains 8 amino acids that direct myristoylation and palmitoylation (Muzumdar et al., 2007). 3 copies of the HA tag were PCR amplified from pTHW (*Drosophila* Genomics Resource Center) and included a 5′ BsrGI restriction site and a 3′ EcoRI restriction site preceded by the TAA stop codon (5′ oligo:TTATGTACAAGTACCCATACGATGTTCCT-GACTATGC; 3′ oligo: TAAGAATTCTTAAGCGTAATCTGGAACGTCATATGGATAGG). pSN20-mtdT (Muzumdar et al., 2007) was digested with BsrGI and EcoRI and the HA PCR fragment was ligated into this vector to generate pSN20-mtdT-3xHA. This vector was then digested with XhoI and partially digested with BamHI and cloned into pQUAST and pUASTattB (Bischof et al., 2007) to generate pQUAST-mtdT-3xHA and pUASTattB-mtdT-3xHA respectively. The mtdT-3xHA reporter in vivo is as good as mCD8-GFP in labeling dendritic and axonal processes, or in labeling imaginal disc tissues. However, it does not label neuronal cell bodies as well as mCD8-GFP as most of the mtdT-3xHA signal is localized to the plasma membrane surface whereas mCD8-GFP, which also localizes to intracellular membranes, allows for the cell soma to be better visualized.

pQUAST-nucLacZ

The nuclear LacZ insert was PCR amplified from *UAS-nucLacZ* genomic flies (Bloomington Stock Center) using oligos genUASFOR and genUASsv40REV. To determine which cloning sites were used in the cloning of UAS-nucLacZ, the PCR fragment was sequenced using UASFOR-SEQ and SV40REV-SEQ. The KpnI/XbaI digested nucLacZ PCR fragment was then ligated into pQUAST.

pQUAST-FLPo

Mammalian codon-optimized FLP recombinase (FLPo; Addgene plasmid 13792) (Raymond and Soriano, 2007) was PCR amplified to include BglII/NotI restriction sites, and cloned into pQUAST to generate pQUAST-FLPo.

pQUAS-DSCP-FLPo

Mammalian codon-optimized FLP recombinase (FLPo; Addgene plasmid 13792) (Raymond and Soriano, 2007) was PCR amplified to include EcoRI/XbaI restriction sites, and cloned into pQUAS-DSCP to generate pQUAS-DSCP-FLPo.

pCa4B2G-QUAS-DSCP-FLPo

The QUAS-DSCP-FLPo-SV40 region was excised from pQUAS-DSCP-FLPo by BamHI digestion, and subcloned into pCa4B2G at the BamHI site that is flanked by gypsy insulators (Markstein et al., 2008). This construct was used for PhiC31-mediated integration into the attP2 locus (Groth et al., 2004).

pUAST > stop > mCD8-GFP

The widely used FLP-Out reporter, *UAS > CD2,y*$^{+}$ *> mCD8-GFP* (Wong et al., 2002) contains non-optimal FRT sites (' > ' represents FRT), which were chosen in order to increase the percentage of small FLP-out clones during FLP-out labeling experiments (G. Struhl, personal communication). As such, in control FLP experiments, there was some variability in the extent of the excision of the 'CD2,y+' cassette in all expected target neurons, presumably due to incomplete excision of the FLP-out cassette. To reduce this variability, optimal FRT sites were used to flank two transcription stops. Direct comparison between *UAS > stop > mCD8-GFP* and *UAS > CD2,y+ > mCD8-GFP* transgenic flies—in test crosses with *GH146-FLP* (Hong et al., 2009) and *elav-GAL4*—verified that the new FLP-out reporter is more effective in removing the cassette between the FRT sites, resulting in decreased variability in *mCD8-GFP* reporter expression (data not shown). Construction of pUAST > stop > mCD8-GFP has been previously described (Hong et al., 2009).

pQUAST > stop > mCD8-GFP

The FRT-Stop-FRT cassette from pUAST > Stop > mCD8-GFP was excised by BglII/NotI digestion. The mCD8-GFP cassette was excised from pQUAST-mCD8-GFP by NotI digestion. The two inserts were ligated into the BglII/NotI sites of the pQUAST vector.

pQUAST-shibire^{ts1}

Shibire^{ts1} was PCR amplified from genomic DNA of *UAS-shibire^{ts1}* transgenic flies (Kitamoto, 2001) using genUASFOR and genUAS-REVsv40 oligos, and ligated into the NotI/KpnI sites of pQUAST. To test for functional transgenic *QUAS-shibire^{ts1}* insertions, we crossed flies containing a particular insertion with flies carrying *ET49-QF*, which broadly expresses QF in many neurons, and then placed the progeny in a 37°C water bath. Flies with a functional *QUAS-shibire^{ts1}* became paralyzed within 20 s, followed by full recovery within 5 min.

pQUAST > stop > shibire^{ts1}

The NotI fragment containing the mCD8-GFP cassette was excised from pQUAS > stop > mCD8-GFP, the vector was blunted, and ligated to a blunted NotI/KpnI *shibire^{ts1}* isolated from pQUAST-shibire^{ts1}. Functional transgenic *QUAS > stop > shibire^{ts1}* insertions were tested by crossing them to *hsFLP122* and *ET49-QF*. The progeny containing all three transgenes were heat shocked at least once during development to excise the > stop > cassette, and then tested as described for *QUAS-shibire^{ts1}*.

pQF-M2ET (Swappable QF Enhancer Trap)

An enhancer trap was constructed that allows recombination mediated cassette exchange (Oberstein et al., 2005). A loxM2 site was inserted immediately following the 5P promoter, and a LoxP site was placed after the selectable *white* marker to generate the vector pDonor-M2, which contains elements in the following order: 5P-Ppromoter-LoxM2-MCS-SV40 terminator-white-LoxP-3P. QF was PCR amplified from pAC-QF adding 5′ EcoRI and 3′ AatII restriction sites, and inserted into the EcoRI/AatII cloning sites of pDonor-M2 to yield pQF-M2ET. Of the 14 original insertions of pQF-M2ET from the initial injection, 5 showed only tracheal expression, 8 showed tracheal expression and expression in additional tissues, and only 1 (*ET40*) showed very minor tracheal expression and high expression in additional tissues (e.g., all imaginal discs, and some adult brain structures). The reason for the tracheal expression is currently unknown. We are generating additional enhancer trap vectors to circumvent the tracheal expression. The *ET40* enhancer trap is inserted into the 5′ upstream region of the *posterior sex combs* (*psc*) gene located at 49E6. The name, cytological location, and associated gene of the pQF-M2ET insertions in Figure S2B are: *#6*, 78A2, *skuld*; *#8*, 47A7, *lola*; #31, 52E11, *Ext2*.

pQF-ET (QF Enhancer Trap)

The QF-SV40polyA fragment was excised from pQF-M2ET,w+ by digestion with EcoRI and BamHI, blunted by Klenow and inserted into blunted pGalW (Brand and Perrimon, 1993) from which the GAL4-hsp70polyA fragment had been excised by NotI digestion. The name, cytological location, and associated gene of the pQF-ET insertions in Figure S2B are: *#11*, 85C3, *CG11033*; *#9*, 49E7, *Su(z)2*; *#12*, 34A10, *snRNA:U2*; *#13*, 44B5, *kermit*; *#14*, 39A5, intergenic; *#10*, 34A10, *CG9426*; *#49*, 70C15, *Hsc70b*.

pUASTattB-QS

The QS cDNA was excised from pAC-QS with Acc65I and NotI, blunted, and ligated into a blunted pUASTattB (Bischof et al., 2007) which had been digested with BglII and KpnI. Transgenic flies with this construct integrated into the attP2 site were used in the experiments shown in Figure 6B.

pattB-QF-SV40

The QF-SV40 cassette from pQF-M2ET was PCR amplified to include EcoRI/NotI restriction sites and inserted into the pattB vector (Bischof et al., 2007).

pattB-QF-hsp70

The QF-hsp70 cassette from pBac-GH146-QF was PCR amplified to include EcoRI/NotI restriction sites and inserted into the pattB vector (Bischof et al., 2007). The hsp70 terminator results in reduced QF expression (in comparison to QF-SV40) and has enabled fly transgenesis using constructs that proved toxic with QF-SV40 (CJP and LL, unpublished results).

pattB-DSCP-QF-SV40

The DSCP from pBPGUw (Pfeiffer et al., 2008) was PCR amplified to include EcoRI/MfeI restriction sites and ligated into the EcoRI site of pattB-QF-sv40.

The previous three vectors contain convenient multi-cloning sites preceding the QF ORF for cloning of promoter/enhancer regions to drive QF expression. These QF constructs can be integrated into the fly genome using ϕC31-mediated integration (Bischof et al, 2007). The DSCP variant can be used if the cloned enhancer region does not contain a promoter (Pfeiffer et al., 2008). These constructs can also be used for convenient isolation of the QF ORF by restriction digestion.

pBS-SK-QS

The QS ORF was PCR amplified from pAC-QS to include EcoRI/XbaI restriction sites, and cloned into pBluescript-SK (Strategene). This construct contains convenient restriction sites before and after QS and can be used for cloning of QS promoter/enhancer constructs or for isolation of the QS ORF.

Expression Studies in Cultured Cells

S2 Cell Transfection

S2 cells (gift of M. Simon, Stanford University) were maintained in Shields and Sang M3 insect medium (Sigma, Catalog # S8398), prepared according to the manufacturer's instructions and supplemented with 10% heat inactivated fetal bovine serum (FBS) and antibiotics (from 100x penicillin/streptomycin stock, Invitrogen, Catalog # 15140). FBS was heat inactivated at 56°C for 30 min. The cells were grown in an air incubator at 25°C. For transfection, 0.4 ml of complete M3 medium containing $5*10^5$ *Drosophila* S2 cells were plated into individual wells of 24-well plates several hours before the transfection. The DNA for transfection was mini-prepped (QIAprep Miniprep kit, QIAGEN, Catalog # 27106), DNA concentrations were determined using the NanoDrop 1000 spectrophotometer (Thermo Scientific), diluted in 10 mM TRIS-HCl pH 7.5, 0.1 mM EDTA to 25 ng/μl, and filtered through a 13-mm 0.2 μm filter (Nalgene, Catalog # 180-1320). For individual transfections, we used 0.2 μg of total DNA (total of 8 μl from 25 ng/μl stocks) including one or more of the following: 25 ng of reporter, 12.5 ng of a transcription factor plasmid and the amount or repressor plasmid that was adjusted according to the molarity of the corresponding transcription factor plasmid to get either equimolar, 3-fold or 5-fold higher molar concentration, as indicated. Each sample also contained 2.5 ng of pP_{AC5C}-hRluc, which was used for normalization of the firefly luciferase signal for each sample (see below) and pBluescript to supplement the total DNA amount to 0.2 μg. The cells were transfected using Effectene (QIAGEN, Catalog # 301425) according to the manufacturer's protocol (for each sample we used: 59 μl EC buffer; 1.6 μl enhancer solution; 4 μl Effectene and 350 μl M3 medium). 12 hr after the addition of transfection mixes to cells, quinic acid was added where indicated from 50x stocks. The starting quinic acid stock solution (250 mg/ml) was prepared from D-(–)-quinic acid (Sigma-Aldrich, 98%, Catalog # 138622) in sterile Milli-Q water and neutralized with NaOH to pH∼7. All other 50x stocks were made from this stock by dilution in water. Cells were lysed 24 hr after the addition of quinic acid (36 hr since the start of transfection), by spinning the 24-well plates for 5′ in a table top centrifuge at ∼1000 g, removing the supernatant by aspiration and incubation with of 200 μl passive lysis buffer (from the Dual Luciferase Reporter Assay System by Promega, Catalog # E1910) with shaking at room temperature for ∼30 min. The lysates were transferred into 1.5 ml tubes and frozen at −80°C. The lysates were analyzed using the Dual Luciferase Reporter Assay System, according to the manufacturer's instructions, and the single tube Turner Biosystems luminometer, model 20/20n. The luminescence light signal for both firefly and Renilla luciferases was collected for 10 s. All samples that were transfected with reporters had at least 100-fold higher signal than the background (lysates from pBluescript-only transfected cells). For each sample "X," the relative luciferase activity (RLA) was calculated according to the following formula:

$$RLA_x = (F_x/R_x)/(\overline{F/R})_{QUAS},$$

where

$$(\overline{F/R})_{QUAS} = \left(\sum_{i=1}^{n} F^i_{QUAS}/R^i_{QUAS}\right)\Big/ n,$$

where n = number of QUAS-only samples; F = Firefly luciferase luminescence signal; R = Renilla luciferase luminescence signal. Each condition was executed at least in triplicate, the average and SEM were determined for each condition, and statistical significance was evaluated using Student's t test. Plasmids used for transfection in S2 cells were: *pUAS-luc2, pQUAS-luc2, pAC-QF, pAC-QS, pAC-GAL4, pAC-GAL80, pAC-hRluc, pBluescript*.

Full suppression was not observed with equimolar ratios of QF and QS (similar lack of full suppression was observed with GAL4/GAL80). This result could be a consequence of transient transfections, where individual cells do not necessarily uptake the same amounts of activator and repressor plasmids. Additionally, somewhat higher QS/QF ratios compared to GAL80/GAL4 ratios are required to reach similar degree of repression. The difference between the two systems probably lies in the specific nature of the individual genes or the corresponding proteins (activity, codon choice, mRNA or protein stability, *etc*.).

HeLa Cell Transfection

HeLa cells (gift of K. Wehner, Stanford University) were maintained in Dulbecco's Modified Eagle Medium (DMEM, Invitrogen, Catalog # 10566), supplemented with 10% FBS and antibiotics (from 100x penicillin/streptomycin stock, Invitrogen, Catalog # 15140) in a 37°C air incubator with 5% CO_2. At least 5 hr before transfection, cells were detached and dissociated from the plate using Triple-express (Invitrogen, Catalog # 12605) and plated into 24-well plates at $7*10^4$ cells in 0.5 ml medium with FBS, but without antibiotics. Cells were transiently transfected using Lipofectamine 2000 (Invitrogen, Catalog # 11668-019), according to the manufacturer's instructions. Plasmid DNA for transfection was prepared as described in the S2 cell transfection protocol above. For each sample we used 0.25 μg DNA (total of 10 μl from 25 ng/μl stocks) including one or more of the following: 50 ng of reporter, 25 ng of a transcription factor plasmid and the amount or repressor plasmid that was adjusted according to the molarity of the corresponding transcription factor plasmid to get either equimolar, 3-fold or 5-fold higher molar concentration, as indicated. Each sample also contained 5 ng of pGL4.75 (hRluc/CMV from Promega), which was used for normalization of the firefly luciferase signal for each sample (see below), and pBluescript to supplement the total DNA amount to 0.25 μg. The DNA was mixed in 50 μl of Opti-MEM (Invitrogen, Catalog # 51985) and combined with another 50 μl of Opti-MEM containing 1 μl of Lipofectamine. The medium containing the transfection mix was replaced with DMEM containing FBS and antibiotics 22 hr after transfection. Where needed, the medium contained quinic acid supplemented from 50x stocks that were made as described in the S2 cell transfection protocol above. 24 hr after the medium was changed, the cells were lysed in 24-well plates and processed as described above in the S2 cell transfection protocol. All samples that were transfected with reporters had at least 100-fold higher signal than the background (lysates from pBluescript-only transfected cells). We have noticed that significantly poorer repression of QF by QS is obtained with shorter transfection times in mammalian cells. Plasmids used for transfection in HeLa cells were: *pUAS-luc2, pQUAS-luc2, pCMV-QF, pCMV-QS, pCMV-GAL4, pCMV-GAL80, pGL4.75* (Promega), *pBluescript*.

Higher QS:QF or GAL80:GAL4 molar ratios are required for effective suppression in HeLa cells compared with *Drosophila* S2 cells. This phenomenon could be due to codon choice and/or differential activity or stability of activators and repressors at different temperatures — 25°C for S2 and 37°C for HeLa.

Drosophila Genetics and Manipulations

Transgenes

Transgenes were generated by standard P-element (Spradling and Rubin, 1982) or PhiC31 integrase-mediated transformation (Groth et al., 2004), as noted in Table S1. All fly transgenes were mapped using splinkerette PCR (Potter and Luo, 2010). When necessary, transgenes were recombined onto the same chromosome using standard meiotic recombination techniques. To check for $Tsc1^{Q600X}$ (Potter et al., 2001) recombinants, a genomic region containing the *Tsc1* point mutation was PCR amplified from genomic DNA using oligos gTsc1-FOR#1 (GCTGCAGTTTGTGGCGAGTG) and gTsc1-REV#1(AACCGATCCCGCTCCATTTC) and cut with the restriction enzyme SnaBI. The SnaBI site was created by the C- > T mutation in the $Tsc1^{Q600X}$ allele. Wild-type *Tsc1* gives an uncut band of 719 bp and the $Tsc1^{Q600X}$ mutant gives bands of sizes 322 bp and 397 bp.

Toxicity of QF

We were unsuccessful in generating *tubP-QF* transgenic animals by either site-directed integration using PhiC31 integrase or P-element mediated transformation. These observations suggest that QF is toxic to flies when highly expressed in a ubiquitous manner or in a particular developmental stage or tissue. We note that in our previous effort to generate *tubP-GAL4*, we encountered similar difficulty in obtaining transgenes from microinjection or transposition. In parallel experiments, we obtained a single *tubP-GAL4* transgene but more than a dozen *tubP-GAL80* transgene insertions (Lee and Luo, 1999). Furthermore, repeated experiments of remobilizing the *tubP-GAL4* transgene resulted in only one additional line on the same chromosome. Both *tubP-GAL4* transgenes are homozygous lethal, but become homozygous viable in the presence of a *tubP-GAL80* transgene, suggesting that high-level ubiquitous expression of GAL4 is toxic. Preliminary results indicate that QF-induced toxicity can also be suppressed by a *tubP-QS* transgene (CJP and LL, unpublished results). We suspect that high-level ubiquitous expression of strong transcription factors such as GAL4 and QF is harmful to flies—probably due to squelching of the transcriptional machinery. It is also possible that high-level expression of QF in some tissues and developmental stages is more harmful than equivalent expression of GAL4.

We are currently experimentally addressing this toxicity issue. As noted in the *Recombinant DNA Construction* section above, terminator choice can make a significant impact on QF expression and toxicity: by exchanging the SV40 terminator with an hsp70 terminator in QF constructs, we were able to generate transgenic animals containing *promoter-QF-hsp70* that previously proved difficult to produce using an SV40 terminator (CJP and LL, unpublished results). In addition, we have generated a mutant QF protein (QFm) that exhibits ~5 fold less activity in S2 transfection assays compared to wild-type QF (BT and LL, unpublished results). We were able to obtain *tubP-QFm* transgenic animals, as well as > 100 QFm enhancer trap lines, but reporter expression levels were not sufficiently strong in many tissues (CJP and LL, unpublished results). We are in the process of isolating a QF variant that drives reporter expression sufficiently well in all tissues. We are also conducting experiments to address the possibility that

a particular developmental stage or a particular tissue is especially sensitive to QF expression. We will report these findings to the fly community in a timely fashion. Nonetheless, we have isolated many QF enhancer trap lines that express strongly in many tissues without adverse effects, including imaginal discs (*ET40-QF*), glia (*ET31-QF*), trachea (*ET14-QF*) and neurons (*GH146-QF* and *ET49-QF*), suggesting that high-level expression of QF is not toxic to many cell types. We further note that the toxicity associated with high-level ubiquitous expression of GAL4 does not prevent the widespread use of the GAL4/UAS system.

Coupled MARCM Analysis of Projection Neuron Lineage

Vials containing approximately 15 males and 25 females were allowed to lay eggs for 8-12 hr. Animals were heat shocked in a 37°C water bath for 1 hr from 0 to 100 hr after egg laying (AEL). Brains from adult animals were dissected 3-5 days after eclosion. The genotype of GH146 coupled MARCM flies is: *hsFLP, QUAS-mtdt-3xHA, UAS-mCD8-GFP* (X); *GH146-QF#53, 82B^{FRT}, tub-QS/ tubP-GAL4, 82B^{FRT}, tubP-GAL80* (III)

Coupled MARCM Analysis of Wing Disc Clones

Vials containing approximately 15 males and 25 females were allowed to lay eggs for 6-8 hr. The progeny were heat shocked in a 37°C water bath for 30 min at 48 ± 3 hr AEL, and dissected 72 ± 3 hr after the heat shock. This 30 min heat shock leads to about 1-2 wild-type coupled MARCM wing clones per disc. (A 1 hr heat shock leads to approximately 5-10 clones per disc.) In control coupled MARCM experiments, coupled MARCM clones in the wing imaginal disc could be visualized in live samples (unfixed/ unstained) as early as 28 hr after the clone-inducing heat shock (clones were induced by a 2 hr heat shock at 60 hr AEL). This observation suggests that perdurance of GAL80 and QS is minimal 28 hr after clone induction.

Quinic Acid Feeding of Flies

Quinic acid containing medium was made as follows: a few holes were made in standard fly medium with wooden sticks, and 0.3 ml of freshly made D-(–)-quinic acid (Sigma-Aldrich, 98%, Catalog # 138622) solution dissolved in water was added per 10 ml of medium. Vials were allowed to air-dry overnight. Quinic acid appears to be stable in food stored for at least a week at 18°C, as judged by its derepression activity (e.g., Figure 2D). For assaying the effect of quinic acid on developing animals, approximately 10 males and 15 females per vial of the genotype *ET40-QF, QUAS-mtdT-3xHA* (II); *82B^{FRT} tubP-QS* (III) were allowed to lay eggs for 6 hr on quinic acid containing medium. Animals fed upon and developed in the quinic acid containing food. Adult flies were imaged within 3 days of eclosion. For assaying the effect of quinic acid feeding on adult flies, approximately 30 adult flies per vial of genotype *ET40-QF, QUAS-mtdT-3xHA* (II); *82B^{FRT} tubP-QS* (III) were allowed to feed on quinic acid medium for the listed times in Figure 2D. For feedings over multiple days, flies were transferred to fresh quinic acid containing food every two days. Starving flies for 24 hr did not lead to increased suppression, suggesting that both well-fed and hungry flies ingested the quinic acid food at similar levels. Flies fed with quinic acid food for up to 10 days exhibited no more derepression than those fed for 5 days.

Imaging and Image Processing

Immunohistochemistry

Confocal images were taken on a LSM 510 Confocal Microscope (Zeiss). The procedures for fixation, immunochemistry and imaging were as described previously (Wu and Luo, 2006). Primary antibodies used were Rat anti-CD8 (Caltag Laboratories, 1:200), Mouse anti-HA (12CA5, 1:100), Rabbit anti-HA (Abcam, 1:100), Rat anti-DNCadherin (DN-EX#8, DSHB, 1:25), Mouse nc82 (DSHB, 1:25), Rabbit anti-β-galactosidase (1:100), Chicken anti-GFP (Aves Labs, 1:100), Mouse anti-acj6 (DSHB, 1:50), Mouse anti-fibrillarin (72B9, 1:20), Rat anti-ELAV (7E8A10, DSHB, 1:100), Mouse anti-Repo (8D12, DSHB, 1:50), Mouse 24B10 (1:25).

Imaging of Adult Flies

Adult flies were imaged on a QImaging Retiga 2000R Cooled Monochrome Digital camera using a Discovery V8 Pentafluor System (Zeiss) with a DS RED filter cube.

GH146 Expression Pattern

Both *GH146-QF* transgenic lines described in this study have approximately equal PNs expression patterns. The major difference is that *GH146-QF#11* expresses QF in fewer ventral PNs than *GH146-QF#53*. *GH146-QF#53* was used for all GH146 coupled MARCM experiments.

Wing Imaginal Disc Quantification

A customized Matlab script was used for the automated calculation of clone size and cell number in confocal stacks. Cell size (area) was calculated by dividing clone area by cell number. Confocal images were initially processed so that only one set of coupled MARCM clones was present in a confocal stack. The clone area was defined by first thresholding the red channel (mtdT-HA staining) or green channel (mCD8-GFP staining) to delineate the clone, and then calculated by summing the number of pixels above the set threshold. Clone areas in the red and green channels were independently calculated throughout the image stack. The z plane containing the largest clone area and two adjacent planes were recorded. The final clone size, cell number and cell size for each image were the average values of these three z planes. For automated counting of cell numbers in the stack, the thresholded red or green clone areas were used as a mask to define the region of interest in the blue channel (anti-fibrillarin staining which marks the single nucleolus in each cell). The algorithm for counting cell numbers was adapted from the ITCN Matlab script by Thomas Kuo and Jiyun Buyn (Center for Bioimage Informatics). The parameters for automated measurements were set according to test measurements of clone area and cell number, which were obtained by manually counting a small randomly selected image set. The obtained numbers were compared for statistical significance using Student's paired t test.

Behavioral Analysis

Olfactory attraction was measured using a modified two choice trap assay (Larsson et al., 2004). 2-3 day old adult flies were starved for 40-42 hr in collection cages containing water moisted Kimwipes. Approximately 100 flies per assay were anaesthetized by cold and placed into a small culture dish at the bottom of a 85 mm x 170 mm, 1000 ml glass jar (Fisher, 02-912-305) covered by a 150 × 15 mm Petri dish (Falcon, 351058) that had three nylon mesh screened holes inserted for ventilation. Odor traps were constructed from 40 ml glass vials (National Scientific B7999-6) to which a custom-built polyethylene top containing a cut pipette tip was securely placed. Traps contained a cotton foam plug to which either 0.5 ml of 1% ethyl acetate (Sigma, > 99.5% purity) dissolved in mineral oil, or mineral oil alone, were added. The behavioral tests were conducted for two hours in a dark humidified room at 34°C.

SUPPLEMENTAL REFERENCES

Berdnik, D., Chihara, T., Couto, A., and Luo, L. (2006). Wiring stability of the adult Drosophila olfactory circuit after lesion. J. Neurosci. *26*, 3367–3376.

Bischof, J., Maeda, R.K., Hediger, M., Karch, F., and Basler, K. (2007). An optimized transgenesis system for Drosophila using germ-line-specific phiC31 integrases. Proc. Natl. Acad. Sci. USA *104*, 3312–3317.

Brand, A.H., and Perrimon, N. (1993). Targeted gene expression as a means of altering cell fates and generating dominant phenotypes. Development *118*, 401–415.

Gerlitz, O., Nellen, D., Ottiger, M., and Basler, K. (2002). A screen for genes expressed in Drosophila imaginal discs. Int. J. Dev. Biol. *46*, 173–176.

Groth, A.C., Fish, M., Nusse, R., and Calos, M.P. (2004). Construction of transgenic Drosophila by using the site-specific integrase from phage phiC31. Genetics *166*, 1775–1782.

Hong, W., Zhu, H., Potter, C.J., Barsh, G., Kurusu, M., Zinn, K., and Luo, L. (2009). Leucine-rich repeat transmembrane proteins instruct discrete dendrite targeting in an olfactory map. Nat. Neurosci. *12*, 1542–1550.

Kitamoto, T. (2001). Conditional modification of behavior in Drosophila by targeted expression of a temperature-sensitive shibire allele in defined neurons. J. Neurobiol. *47*, 81–92.

Lai, S.L., and Lee, T. (2006). Genetic mosaic with dual binary transcriptional systems in Drosophila. Nat. Neurosci. *9*, 703–709.

Larsson, M.C., Domingos, A.I., Jones, W.D., Chiappe, M.E., Amrein, H., and Vosshall, L.B. (2004). Or83b encodes a broadly expressed odorant receptor essential for Drosophila olfaction. Neuron *43*, 703–714.

Lee, T., and Luo, L. (1999). Mosaic analysis with a repressible cell marker for studies of gene function in neuronal morphogenesis. Neuron *22*, 451–461.

Markstein, M., Pitsouli, C., Villalta, C., Celniker, S.E., and Perrimon, N. (2008). Exploiting position effects and the gypsy retrovirus insulator to engineer precisely expressed transgenes. Nat. Genet. *40*, 476–483.

Muzumdar, M.D., Tasic, B., Miyamichi, K., Li, L., and Luo, L. (2007). A global double-fluorescent Cre reporter mouse. Genesis *45*, 593–605.

Oberstein, A., Pare, A., Kaplan, L., and Small, S. (2005). Site-specific transgenesis by Cre-mediated recombination in Drosophila. Nat. Methods *2*, 583–585.

Pfeiffer, B.D., Jenett, A., Hammonds, A.S., Ngo, T.T., Misra, S., Murphy, C., Scully, A., Carlson, J.W., Wan, K.H., Laverty, T.R., et al. (2008). Tools for neuroanatomy and neurogenetics in Drosophila. Proc. Natl. Acad. Sci. USA *105*, 9715–9720.

Potter, C.J., Huang, H., and Xu, T. (2001). Drosophila Tsc1 functions with Tsc2 to antagonize insulin signaling in regulating cell growth, cell proliferation, and organ size. Cell *105*, 357–368.

Potter, C.J., and Luo, L. (2010). Splinkerette PCR for mapping transposable elements in Drosophila. PLoS ONE. 10.1371/journal.pone.0010168.

Raymond, C.S., and Soriano, P. (2007). High-efficiency FLP and PhiC31 site-specific recombination in mammalian cells. PLoS ONE *2*, e162.

Raymond, C.S., and Soriano, P. (2007). High-efficiency FLP and PhiC31 site-specific recombination in mammalian cells. PLoS ONE *2*, e162.

Spradling, A.C., and Rubin, G.M. (1982). Transposition of cloned P elements into Drosophila germ line chromosomes. Science *218*, 341-347.

Wong, A.M., Wang, J.W., and Axel, R. (2002). Spatial representation of the glomerular map in the *Drosophila* protocerebrum. Cell *109*, 229-241.

Wu, J.S., and Luo, L. (2006). A protocol for dissecting *Drosophila melanogaster* brains for live imaging or immunostaining. Nat. Protoc. *1*, 2110-2115

Zong, H., Espinosa, J.S., Su, H.H., Muzumdar, M.D., and Luo, L. (2005). Mosaic analysis with double markers in mice. Cell *121*, 479-492

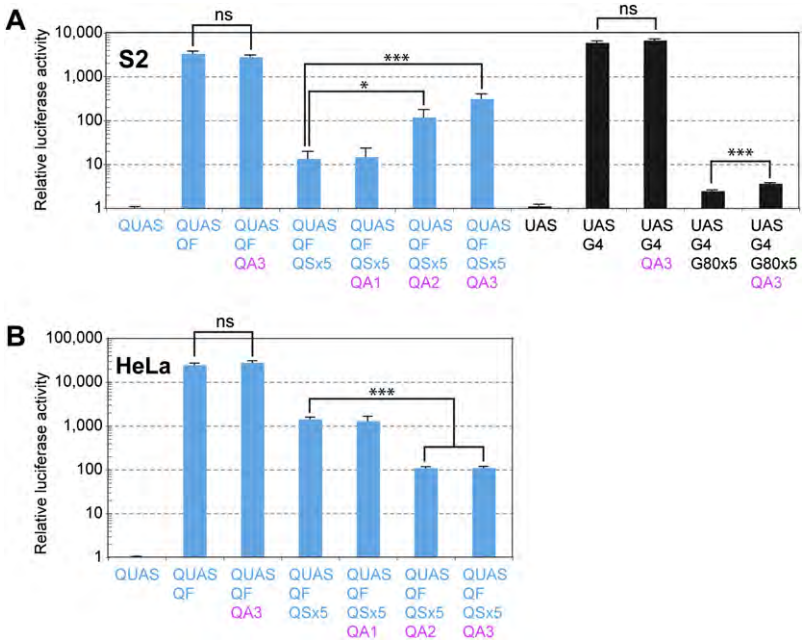

Figure S1. The Effect of Quinic Acid on Transiently Transfected *Drosophila* and Mammalian Cells, Related to Figure 1

(A) The effect of quinic acid on transiently transfected *Drosophila* S2 cells. Relative luciferase activity (normalized as described in Extended Experimental Procedures) is plotted on a logarithmic scale on the *y* axis, with QUAS-luc2 alone set to 1. Quinic acid (QA) was added where indicated to the final concentration of: QA1 = 12.5 μg/ml; QA2 = 250 μg/ml; QA3 = 5 mg/ml. All data are presented as average + SEM. Statistical significance was evaluated using Student's t test; ns, not significant; *$p < 0.05$; ***$p < 0.001$. QA, at the highest concentration tested, results in ~23-fold re-activation of QUAS, compared to the control sample with QUAS, QF and 5xQS. At this high concentration, QA has no effect on QF activation of QUAS or Gal4 activation of UAS, and it has a small but significant effect on GAL80 repression of GAL4: it derepresses GAL4 by ~1.5-fold. Plasmids used for transfections are noted below the *x* axis. QUAS, *pQUAS-luc2* reporter; QF, *pAC-QF*; QS, *pAC-QS*; x5, five-fold molar excess of QS over QF.

(B) The effect of quinic acid on transiently transfected human HeLa cells. The data are presented, and statistical significance was evaluated, as in (A). QA has no effect on QF-dependent transcription of QUAS, but in the presence of QF and 5xQS, it further significantly suppresses QUAS activation by ~13-fold at the two higher QA concentrations tested. Explanations and abbreviations as in (A) except: QF, *pCMV-QF*; QS, *pCMV-QS*.

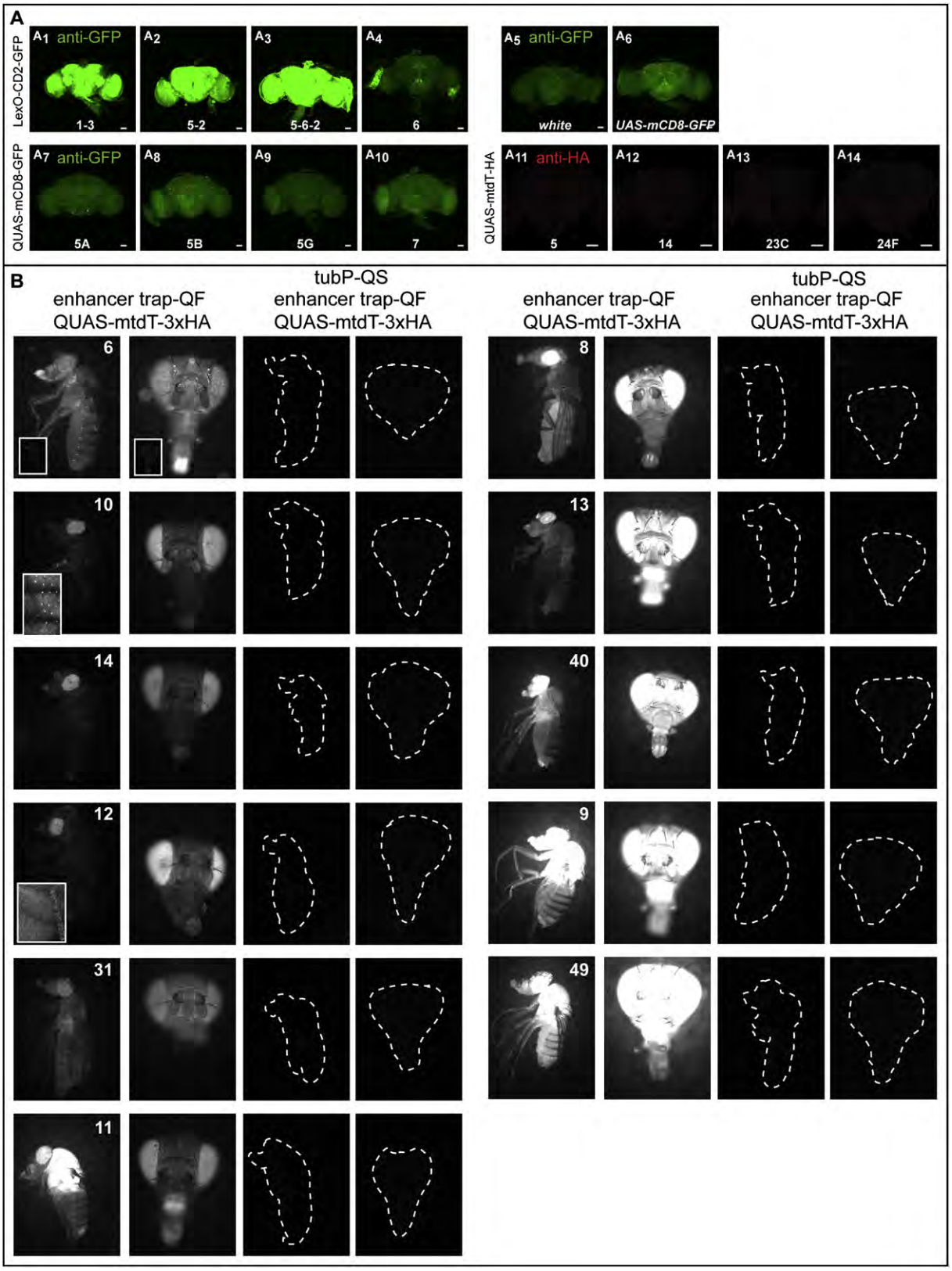
A
LexO-CD2-GFP
A1 anti-GFP
1-3
A2
5-2
A3
5-6-2
A4
6
A5 anti-GFP
white
A6
UAS-mCD8-GFP
QUAS-mCD8-GFP
A7 anti-GFP
5A
A8
5B
A9
5G
A10
7
QUAS-mtdT-HA
A11 anti-HA
5
A12
14
A13
23C
A14
24F
B
enhancer trap-QF
QUAS-mtdT-3xHA
tubP-QS
enhancer trap-QF
QUAS-mtdT-3xHA
enhancer trap-QF
QUAS-mtdT-3xHA
tubP-QS
enhancer trap-QF
QUAS-mtdT-3xHA
6
8
10
13
14
40
12
9
31
49
11

Figure S2. Further Characterization of the Q System In Vivo, Related to Figure 2

(A) Comparison of basal expression levels for *UAS*-, *lexAO*- and *QUAS*-reporter transgenes in the adult *Drosophila* brain. All images show maximum z-projections of confocal stacks. A_1-A_{10} show anti-GFP antibody staining of adult brains of: (A_5) a *white*^{1118} control fly, (A_6) a commonly used *UAS-mCD8-GFP* fly (Lee and Luo, 1999), (A_1-A_4) four independent insertions of *lexAO-CD2-GFP* (Lai and Lee, 2006), (A_7-A_{10}) four independent insertions of *QUAS-mCD8-GFP* (this study). A_{11}-A_{14} show anti-HA staining of adult brains for four independent insertions of *QUAS-mtdT-HA* (this study).

All brains that were stained against GFP (A_1-A_{10}) were processed using identical staining and imaging conditions, which were set such that the anti-GFP signal in control animals (*GH146-GAL4* + *UAS-mCD8-GFP*) was fully saturated (not shown). All brains that were stained against HA (A_{11}-A_{14}) were processed using identical conditions. Imaging conditions were set such that the anti-HA signal in control animals (*GH146-QF* + *QUAS-mtdT-HA*) was fully saturated (not shown). All brains were heterozygous for the driver and reporter transgenes. Line numbers or genotypes are indicated on the bottom of each image. Scale bar = 50 μm.

(B) Expression of QF enhancer trap lines and their suppression by ubiquitous expression of QS. Fluorescence images of adult flies of QF enhancer traps (*ET*) lines expressing the same *QUAS-mtdT-HA* reporter are shown. *ET* line numbers are indicated in the first panel for each set of four panels. All images were taken at the same exposure (400 ms), except for *ET6-QF*, which was taken with a longer exposure. Inset panels for *ET6-QF* show the same images at the 400 ms exposure. Inset panels for *ET10-QF* and *ET12-QF* are higher magnifications of the abdomen showing that each bristle socket is labeled. The animals are ordered from lowest expressing line (*ET6-QF*) to highest expressing line (*ET49-QF*) from top to bottom and continuing to the right column. Expression of each *ET* line can be suppressed by *tubP-QS*, although occasionally a few cells remained labeled with *ET49-QF* (not shown). White outlines mark the positions of the adult flies and magnified heads in the presence of *tubP-QS*. These QF enhancer trap lines exhibited no gross defects caused by QF expression. Line *ET10-QF* exhibited a crumpled wing, but this is likely due to a mutational insertion - other QF enhancer trap lines expressing more highly in similar tissues appeared normal (e.g., *ET40-QF, ET9-QF, ET49-QF*).

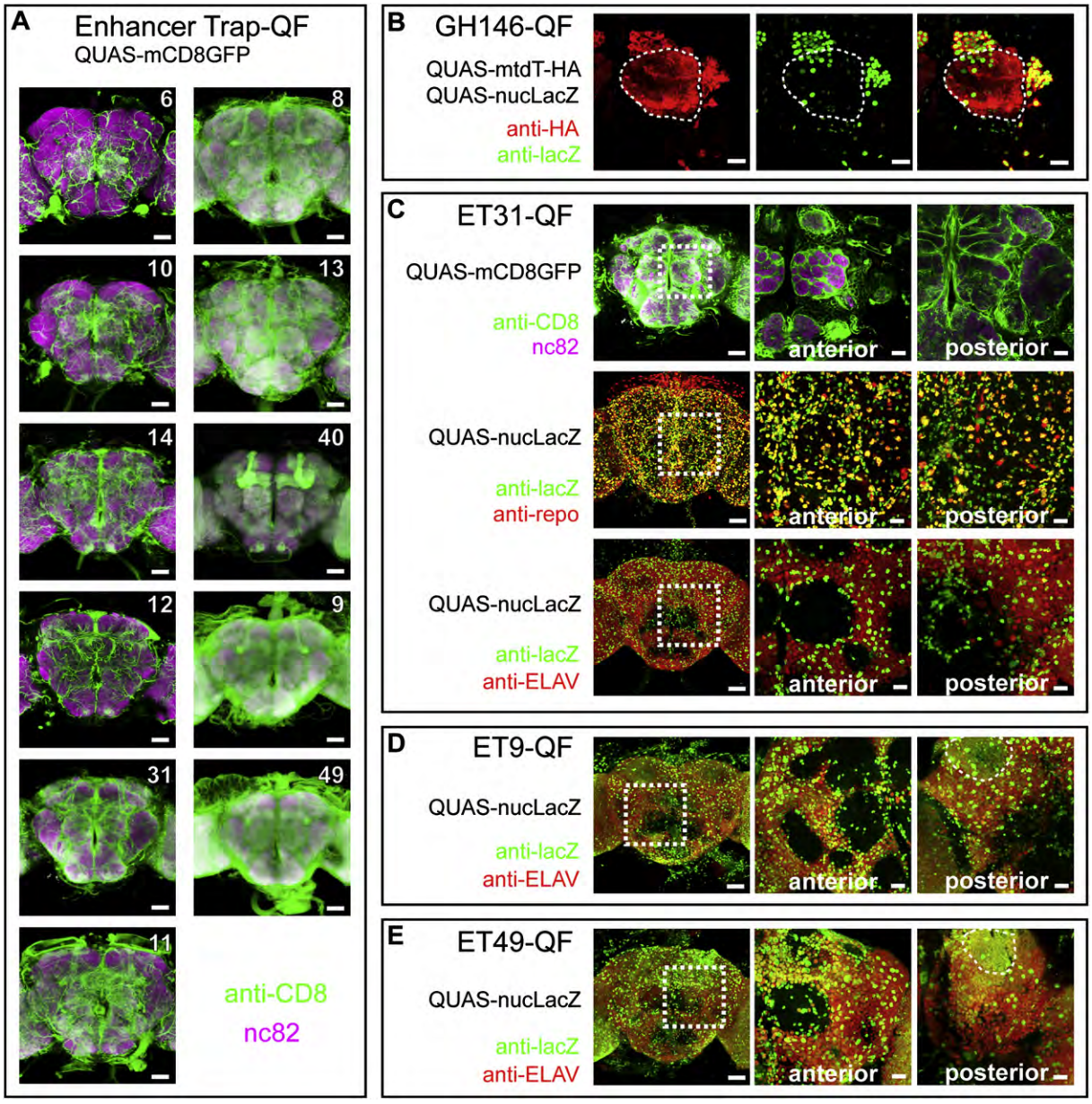

Figure S3. Expression of QF Enhancer Trap Lines in the Adult Brain, Related to Figure 2

(A) Representative limited z-projections of confocal stacks of whole mount *Drosophila* brains containing a QF enhancer trap (line number indicated on top right) and *QUAS-mCD8GFP*. The brains were immunostained for a general neuropil marker (monoclonal antibody nc82) in magenta, and for mCD8 in green. The QF enhancer trap line number is indicated within each panel. The lines are organized as in Figure S2B. All lines except *ET40-QF* express in trachea to varying degrees. Notable expression patterns are: *ET6-QF, ET10-QF, ET14-QF*, and *ET12-QF*—mostly trachea with few neurons; *ET31-QF*—ensheathing glia (see Figure S3C); *ET11-QF*—AL, CC, and MB; *ET8-QF*—general expression in brain tissues, especially in the AL, CC, MB, OL and SOG; *ET13-QF*—expression throughout the brain; *ET40-QF*—AL, MB, OL and SOG; *ET9-QF* and *ET49-QF*—strong expression throughout the brain including AL, CC, MB and SOG. Full confocal stack files available upon request. Abbreviations: AL, antennal lobe; CC, central complex; MB, mushroom bodies; OL, optic lobe; SOG, subesophageal ganglion. Scale bars: 50 μm.

(B) *GH146-QF* labels olfactory PNs. The PN nuclei are labeled by *GH146-QF* driven *QUAS-nuclear-LacZ* (nucLacZ, anti-LacZ in green) and PN morphology is outlined by *QUAS-mtdT-HA* (anti-HA in red) transgenes. Note that all red neurons contain green nuclei. There are some scattered green-only cells (LacZ-positive, mtdT-HA-negative). As nuclear-LacZ is likely a more stable marker than mtdT-HA (our unpublished observations), the green-only cells might represent those that expressed *GH146-QF* transiently during development. Dotted lines represent the antennal lobes, which contain PN dendrites. Scale bars: 20 μm.

(C) *ET31-QF* labels ensheathing glia. (TOP) Limited z-projection confocal images of *ET31-QF* driving mCD8-GFP expression (left panel). The labeled cells ensheath neuronal tissues, such as the glomeruli of the antennal lobe (anterior section, middle panel) and mushroom body lobes (posterior section, right panel). (MIDDLE) Full z-projection confocal image of *ET31-QF* driving nuclear LacZ expression. The brain was stained against lacZ (green) and against the glial marker Repo (red); cells expressing both markers appear yellow (left panel). Limited z-projection confocal images of anterior (middle panel) and posterior (right panel)

sections show that many Repo-positive cells are labeled by *ET31-QF*. (BOTTOM) Full z-projection confocal image of *ET31-QF* driving nuclear LacZ expression (green), co-stained with an antibody against the neuronal marker ELAV (red); cells expressing both markers appear yellow (left panel). Limited z-projection confocal images of anterior (middle panel) and posterior (right panel) sections show that *ET31-QF* rarely labels ELAV-positive cells. Cells labeled by *ET31-QF* that are both Repo-negative and ELAV-negative most likely represent tracheal cells. The white boxes in the left panels show the brain regions that are magnified in the middle and right panels. Scale bars: 50 μm for left panels; 20 μm for middle and right panels.

(D and E) Enhancer trap lines *ET9-QF* and *ET49-QF* label many neurons. Full z-projections of confocal images of *Drosophila* brains containing *ET9-QF* or *ET49-QF* driving nuclear LacZ expression. The brains were stained against lacZ (green) and against the neuronal marker ELAV (red) (left panels). Limited z-projection confocal images of anterior (middle panels) and posterior (right panels) sections show that many neurons are labeled by these *ET* lines. Mushroom body neurons are outlined in images on the right. Scale bars: 50 μm for left panels; 20 μm for middle and right panels.

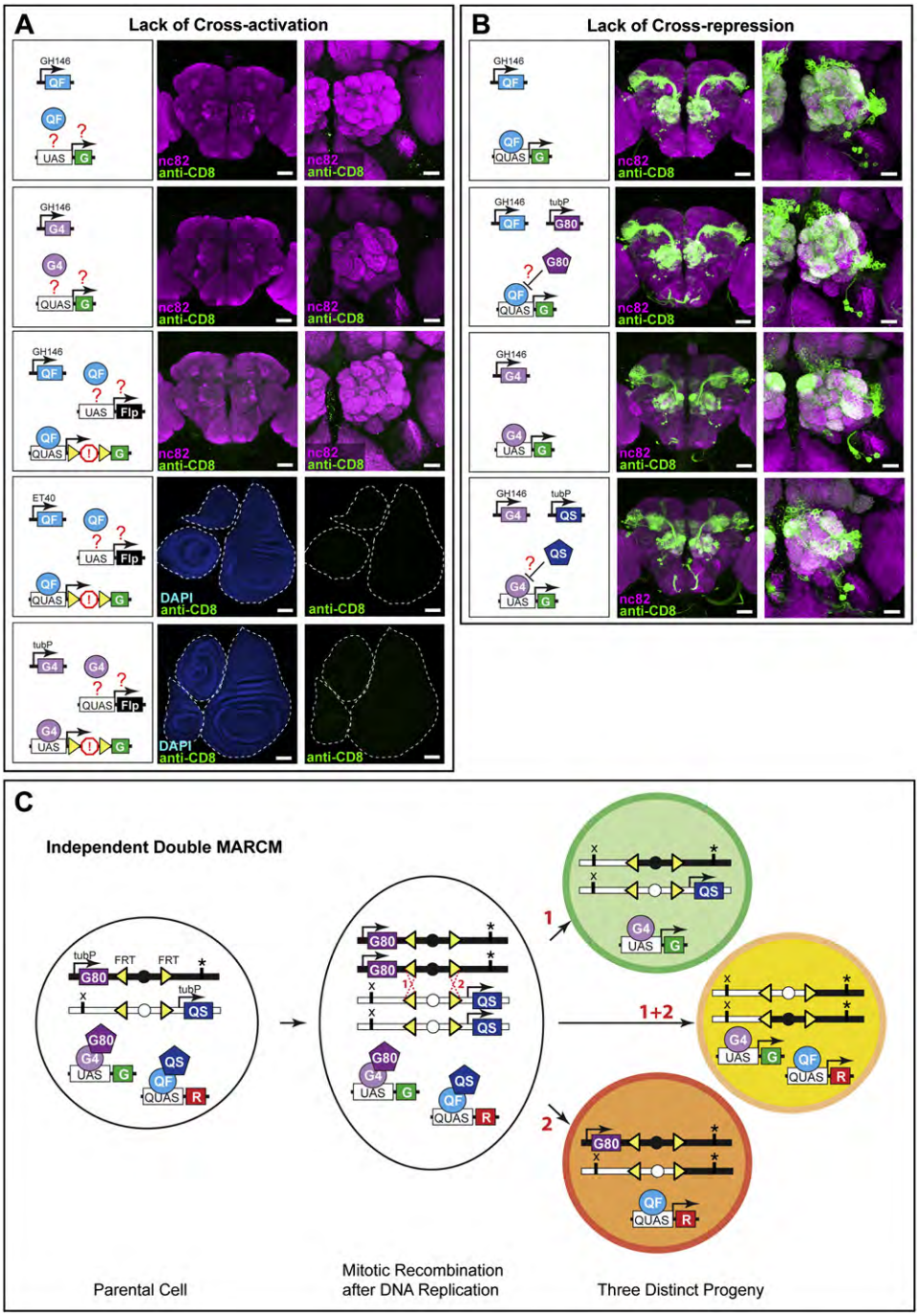

Figure S4. The QF and GAL4 Systems Do Not Cross-Activate or Cross-Repress In Vivo, Related to Figure 3

(A) QF and GAL4 systems do not cross-activate in vivo.

(First to Third row) Representative confocal projections of whole mount *Drosophila* brains immunostained for a general neuropil marker (monoclonal antibody nc82) in magenta, and for mCD8 in green. The genotypes are represented by the schematics in the left panels. Higher magnification images centered at the antennal lobe are shown in the right panels. Staining and imaging conditions were similar to those of Figure 2A. Scale bars: 50 μm for middle panels; 20 μm for right panels.

(First row) *GH146-QF* expression does not activate a *UAS-mCD8-GFP* reporter.

(Second row) *GH146-GAL4* expression does not activate a *QUAS-mCD8-GFP* reporter.

(Third row) *GH146-QF* expression does not activate *UAS-FLP* since mCD8-GFP was not expressed from the *QUAS > stop > mCD8-GFP* reporter. Yellow triangle or '>', FRT site; '!' or 'stop', transcriptional stop.

(Fourth and Fifth row) Representative confocal projections of wing imaginal discs immunostained for mCD8 in green and nuclei using DAPI in blue. The genotypes

are represented by the schematics in the left panel. Staining and imaging conditions were similar to those of Figure 5 and S6C. Scale bars: 50 μm. Yellow triangle, FRT site; '!', transcriptional stop.

(Fourth row) QF expression throughout the wing imaginal disc (driven by *ET40-QF*) does not activate *UAS-FLP* since mCD8-GFP was not expressed from the *QUAS > stop > mCD8-GFP* reporter. 50 wing imaginal discs were examined. Eye imaginal discs (n = 30) also showed no reporter expression (not shown). Yellow triangle or '>', FRT site; '!' or 'stop', transcriptional stop.

(Fifth row) GAL4 expression throughout the wing imaginal disc (driven by *tubP-GAL4*) does not activate *QUAS-FLP* since mCD8-GFP was not expressed from the *UAS > stop > mCD8-GFP* (right panel) reporter. 20 wing imaginal discs were examined. Eye imaginal discs (n = 6) also showed no reporter expression (not shown). Yellow triangle or '>', FRT site; '!' or 'stop', transcriptional stop.

(B) QF and GAL4 systems do not cross-repress in vivo.

Representative confocal projections of whole mount *Drosophila* brains immunostained for a general neuropil marker (monoclonal antibody nc82) in magenta, and for mCD8 in green. The genotypes are represented by the schematics on the left. Higher magnification images centered at the antennal lobe are shown on the right. Comparison of first and second rows indicates that *GH146-QF* expression, as reported by *QUAS-mCD8-GFP*, is not affected by ubiquitous expression of GAL80. Comparison of third and fourth rows indicate that *GH146-GAL4* expression, as reported by *UAS-mCD8-GFP*, is not affected by ubiquitous expression of QS. All experimental conditions (staining protocol, antibody concentrations, number of brains per staining, imaging conditions) were identical. Scale bars: 50 μm for middle panels; 20 μm for right panels.

(C) Schematic of independent double MARCM. *tubP-GAL80* and *tubP-QS* are placed on two different chromosome arms. Two types of mitotic recombination events (1 and 2) are independent of each other and result in differently labeled progeny. Cells homozygous for a single mutation (x or *) are singly colored green or red, respectively, while cells homozygous for both mutations appear yellow. Additional *UAS* or *QUAS* transgenes can be included into the scheme, so that progeny containing active GAL4 or QF can express additional markers or effector genes. Centromeres are represented as circles on the chromosomes. This type of manipulation will be useful for studying gene function in cell-cell interactions and in comparing phenotypes of single and double mutants in the same animal.

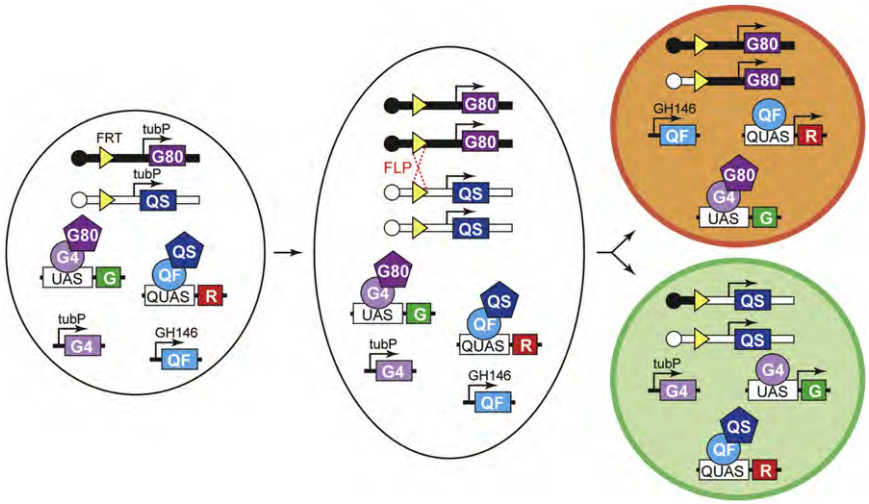

Figure S5. Schematic for Coupled MARCM for PN Lineage Analysis, Related to Figure 4

Mitotic recombination followed by specific chromosome segregation produces two distinct progeny. One progeny is devoid of the QS transgene and is therefore capable of expressing a red fluorescent protein (R, *QUAS-mtdT-HA*) via *GH146-QF* in PNs. The other progeny is devoid of the *GAL80* transgene and is therefore capable of expressing a green fluorescent protein (G, *UAS-mCD8-GFP*) via *tubP-GAL4* in any cell that is the sibling of the red cell above. FLP expression during development is mediated by a 1 hr heat-shock induction of a *hs-FLP* transgene (not diagrammed).

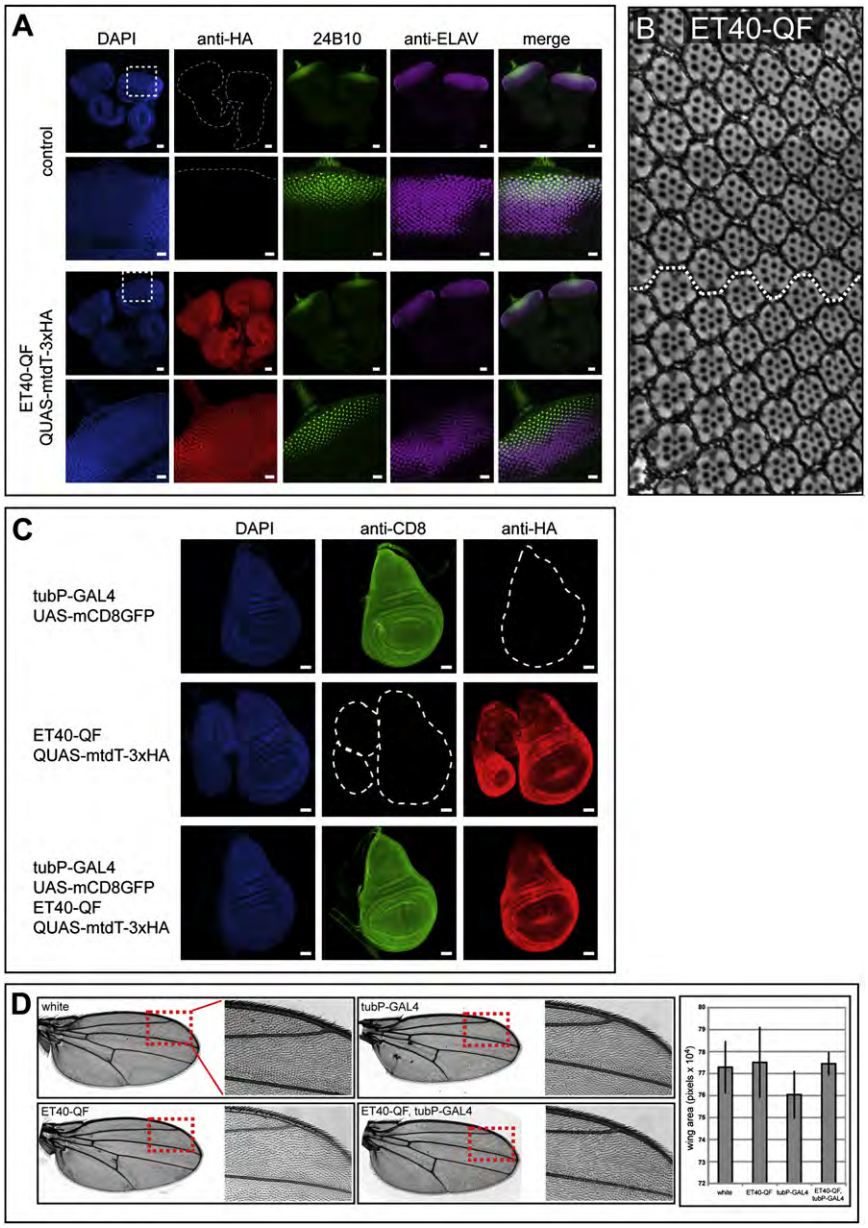

Figure S6. Expression of QF, or Coexpression of QF and GAL4, Does Not Affect Imaginal Disc Development, Related to Figure 5

(A) Eye disc differentiation is not affected by QF expression. Third instar eye imaginal discs were stained for nuclei (DAPI), HA (from *QUAS-mtdT-HA*), 24B10 (photoreceptor specific marker), and ELAV (neuronal differentiation marker) to monitor normal differentiation. Marker expression appears indistinguishable in eye imaginal discs that express QF throughout eye disc development (*ET40-QF*, rows three and four) and in control wild-type imaginal discs (Canton S, rows one and two). Scale bars: 50 μm for rows 1 and 3; 20 μm for rows 2 and 4. Rows 2 and 4 show higher magnification images of eye discs from Rows 1 and 3.

(B) Adult eye section of *ET40-QF* animals, which expressed QF throughout eye disc development, exhibits no defects. The dashed line labels the dorsal/ventral equatorial border.

(C) Expression of QF and GAL4 together in wing imaginal discs does not affect expression levels of QF and GAL4 reporters. Third instar eye imaginal discs of the genotypes listed on the left were stained for nuclei (DAPI), mCD8 (from *UAS-mCD8-GFP*), and HA (from *QUAS-mtdT-HA*). Expression of QF does not affect the levels of GAL4-mediated reporter expression (compare anti-mCD8 signal in top row and third row), and expression of GAL4 does not affect QF-mediated reporter expression (compare anti-HA signal in second and third rows). To limit experimental variability during immunostaining, 15 wings discs for each of the three genotypes were stained together in the same tube. Scale bars: 50 μm.

(D) Wing disc expression of QF, or coexpression of QF and GAL4, does not affect adult wing morphogenesis. Light microscope images of whole adult wings and magnified images of the anterior wing regions are shown for the genotypes listed on top. The development and morphogenesis of the adult wing (as monitored by vein pattern, bristle orientation and wing size) is unaffected by expression of QF, GAL4, or QF+GAL4. For each genotype, we examined at least 20 wings and all wings appeared normal with the exception that one out of 46 wings in the QF+GAL4 condition exhibited an incomplete L3-4 cross vein. Wing sizes were calculated in ImageJ by measuring the wing area (excluding the wing hinge). No significant differences in wing size were found. Error bars are ± SEM.

Logic Gate	A-GAL4 B-QF	Additional Transgenes Required
A OR B		UAS-R, QUAS-R
B NOT A		UAS-QS, QUAS-R
A NOT B		*QUAS-GAL80*, UAS-R
A AND B		1) UAS-FLP, QUAS>stop>R 2) QUAS-FLP, UAS>stop>R
NOT A		UAS-QS, QUAS-R, (*B= tubP*)
NOT B		*QUAS-GAL80*, UAS-R, (A= tubP)
A → B		*tubP>QF>* , UAS-FLP, QUAS-R
B → A		*tubP>GAL4>*, QUAS-FLP, UAS-R
A XOR B		UAS-QS, *QUAS-GAL80*, UAS-R, QUAS-R
A NOR B		*tubP>R>* , UAS-FLP, QUAS-FLP
A NAND B		*tubP>R>QF*, QUAS-FLP, UAS-QS, QUAS-R
	A-FLP B-QF	
A XNOR B		*tubP>GAL4>* , *QUAS>GAL80>GAL4*, UAS-R

Figure S7. Reporter Expression Patterns Derived from Logic Gates of QF and GAL4 Expression Patterns, Related to Figure 6

Grey squares represent the original expression pattern of GAL4 or QF (top line), or the reporter (R) expression resulting from the listed logic gate. The transgenes required for the intersectional logic gates are listed in the right column. Not listed here are four remaining logic gates (A, B, FALSE, TRUE), which do not create new expression patterns. Transgenes not yet constructed are italicized. Although there are multiple ways to construct each logic gate, we show only one for each except for the AND gate, for which we have experimentally demonstrated two alternative methods. ' > ' represents an FRT site.

Table S1. Q System Resources—Transgenics and Recombinants Generated in This Study

Name	Chromosome [a]
QUAS reporters	
QUAS-mCD8-GFP	X, 2nd, 3rd
QUAS-mtdTomato-3xHA	X, 2nd, 3rd
QUAS-nucLacZ	X, 2nd, 3rd
QUAS-FLPo	X, 2nd, 3rd, 3rd (attP2 [b])
QUAS>stop>mCD8-GFP	2nd, 3rd
QUAS-shibire^{ts1}	X, 2nd, 3rd
QUAS>stop>shibire^{ts1}	3rd
QF lines:	
GH146-QF	2nd, 3rd
ET9-QF	2nd
ET31-QF	2nd
ET40-QF	2nd
ET49-QF	3rd
QS lines:	
tubP-QS	X, 2L, 2R, 3L, 3R [c]
UAS reporters:	
UAS-QS	3rd (attP2, ZH-attP-86Fa [d])
UAS>stop>mCD8-GFP	2nd, 3rd
UAS-mtdTomato-3xHA	3rd (ZH-attP-86Fa)
Recombinant Transgenic Animals:	
GH146-QF recombinants:	
GH146-QF#53, QUAS-mCD8-GFP	3rd
GH146-QF#53, QUAS-mtdT-3xHA	3rd
GH146-QF#11, UAS>stop>mCD8-GFP	2nd
GH146-QF#11; UAS>stop>mCD8-GFP	2nd, 3rd
GH146-QF#11, UAS-FLP	2nd
y, w; Pin/CyO; UAS-FLP, GH146-QF#53	3rd
GH146-QF#11; QUAS-FLPo^{attP2}	2nd, 3rd
GH146-QF#53 FRT^{82B}	3rd
GH146-QF#53, FRT^{82B}, tubP-QS#9B	3rd
GH146-QF#53, FRT^{82B}, tubP-QS#21	3rd
ET40-QF recombinants:	
ET40-QF, QUAS-mCD8-GFP	2nd
ET40-QF, QUAS-mtdT-3xHA	2nd
Stocks for MARCM analysis:	
tubP-QS#4, 40A^{FRT}	2nd
FRT^{82B}, tubP-QS#9B	3rd
FRT^{82B}, tubP-QS#21	3rd
tubP-GAL4, FRT^{82B} /TM6B	3rd
y, w; Pin/CyO; tubP-GAL4, FRT^{82B} /TM6B	3rd
y, w; Pin/CyO; tubP-GAL4, FRT^{82B}, tubP-GAL80/TM6B	3rd
y, w; Pin/CyO; tubP-GAL4, FRT^{82B}, tubP-GAL80, Tsc1^{Q600X} /TM6B	3rd
y, w; ET40-QF, QUAS-mtdT-3xHA; FRT^{82B}, tubP-QS#9	2nd, 3rd
y, w; ET40-QF, QUAS-mtdT-3xHA; FRT^{82B}, tubP-QS#21	2nd, 3rd
hsFLP, QUAS-mtdT-3xHA, UAS-mCD8-GFP	X
UAS-mCD8-GFP, QUAS-mtdT-3xHA; Pin/CyO	X
QUAS-mCD8-GFP#5B, tubP-GAL4/TM6B	3rd
acj6-GAL4, UAS-mCD8-GFP/FM7c; Pin/CyO	X
y, w; FRT^{82B}, Tsc1^{Q600X}/TM6B	3rd

[a] See Schematic for cytological locations of insertion sites for a subset of these transgenes.
[b] See (Groth et al., 2004; Markstein et al., 2008).
[c] These transgenes have been recombined with common FRTs on respective chromosomes.
[d] See (Bischof et al., 2007).

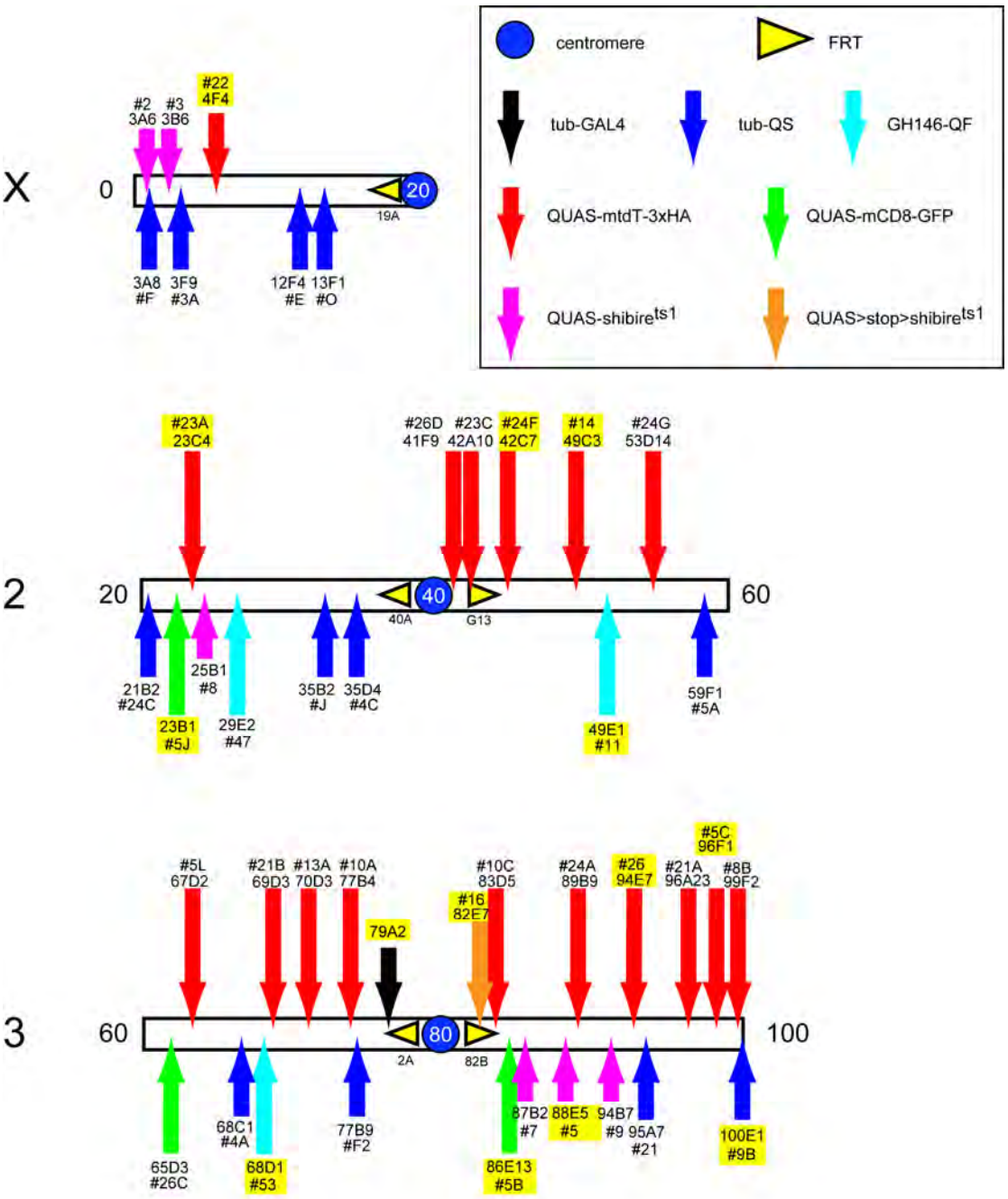

Cytological Locations of Mapped Transgenes, Schematic Associated with Table S1

The locations of mapped transgenes are indicated on five major chromosome arms of *Drosophila,* with each insertion characterized by its cytological location and its transgenic line number (symbols are explained in the legend, top right). The specific lines used in this study are highlighted in yellow.